

PAUL SCHERRER INSTITUT



Zurab Guguchia :: LMU :: Paul Scherrer Institut

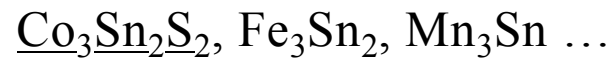
Tunable Berry Curvature Through Magnetic Phase Competition in a
Topological Kagome Magnet $\text{Co}_3\text{Sn}_2\text{S}_2$

Alma mater: Tbilisi State University, Georgia

A solid grey square is positioned on the left side of the slide.

Exploring the interplay between **magnetic order** and **electronic topology** is an emerging frontier in condensed matter physics!

Several **kagome magnets** have appeared as the most promising platforms:



Outline

- Background on Weyl semimetals.
- Weyl nodes, flat band diamagnetism and anomalous hall in $\text{Co}_3\text{Sn}_2\text{S}_2$.
- Homogeneous ferromagnetic ground state in $\text{Co}_3\text{Sn}_2\text{S}_2$.
- Volume wise magnetic competition at high temperatures in $\text{Co}_3\text{Sn}_2\text{S}_2$.
- Magnetic competition driven thermal evolution of anomalous hall conductivity.
- Symmetry analysis - DFT - μSR local field simulation - Neutron diffraction.
- Pressure and magnetic field tuning of the magnetic competition in $\text{Co}_3\text{Sn}_2\text{S}_2$.

PAUL SCHERRER INSTITUT



Collaborators

PAUL SCHERRER INSTITUT



Laboratory for Muon Spin Spectroscopy

Joel Verezhak

Hubertus Luetkens

Alex Amato

Robert Scheuermann

Rustem Khasanov

Gediminas Simutis

Laboratory for Developments and Methods

Gawryluk Dariusz Jakub

Ekaterina Pomjakushina

Laboratory for Neutron Scattering and Imaging

Vladimir Pomjakushin

Lukas Keller



**PRINCETON
UNIVERSITY**

Zahid Hasan

Jiaxin Yin

Ilya Belopolski

Tyler Cochran

Songtian Zhang

Guoqing Chang



**University of
Zurich** ^{UZH}

Titus Neupert

Stepan Tsirkin



Huibin Zhou

Shuang Jia



SWISS NATIONAL SCIENCE FOUNDATION

Discovery of a Weyl fermion semimetal

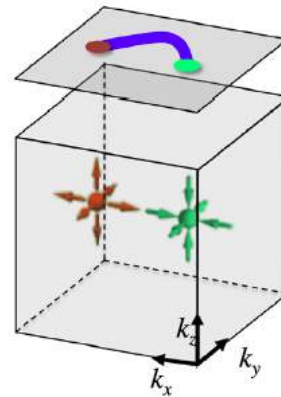
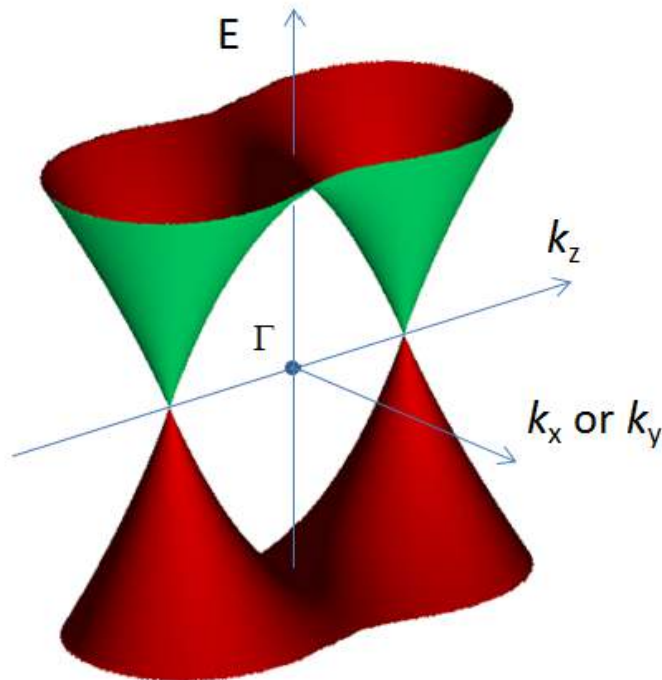


WFs were predicted in 1929 by Hermann Weyl.

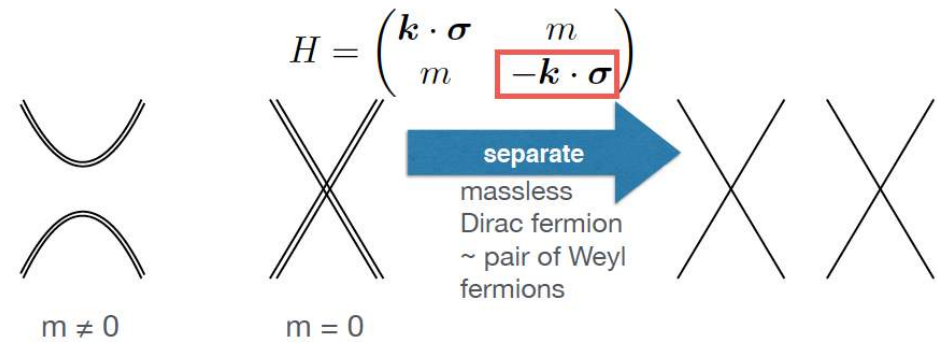
Exp. observation in TaAs in 2015 (Science 349, 613-617 (2015)).

Nat. Comm. 6, 7373 (2015). Phys. Rev. X 5, 011029 (2015). Nature **527**, 495 (2015).

Bulk "Weyl cones"



Weyl nodes in the bulk:

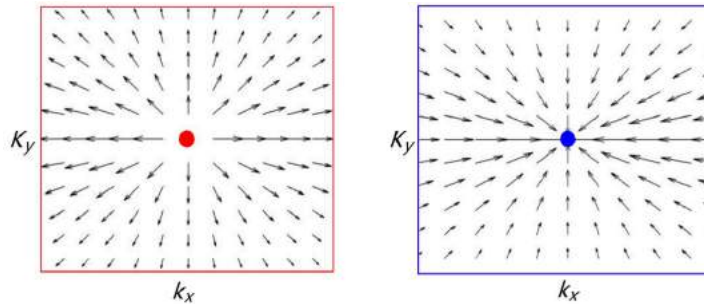


How do they compare with 3D topological insulators?
 topological insulators: boring bulk, interesting surface.
 Weyl semimetals: interesting bulk and surface.

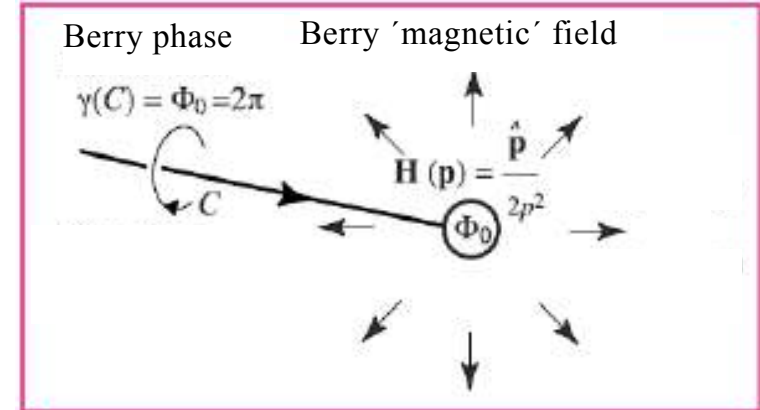
Princeton, Beijing, Oxford, Villigen
 ARPES exp. on TaAs, NbAs, TaP

Berry curvature

Chirality: **sources** and **sinks** of Berry curvature



Chern number = ± 1
 i.e., monopole of Berry curvature in momentum space



Key quantity: $\vec{\Omega}(\mathbf{k}) = \nabla_{\mathbf{k}} \times \vec{A}(\mathbf{k}) = \nabla_{\mathbf{k}} \times i \langle \mathbf{u}_{n\mathbf{k}} | \nabla_{\mathbf{k}} | \mathbf{u}_{n\mathbf{k}} \rangle$
 $\vec{A}(\mathbf{k})$: Berry connection, $\mathbf{u}_{n\mathbf{k}}$: periodic part of Bloch function
can be viewed as magnetic field in k-space

[Sundaram & Niu, et.al, PRB (1999); Jungwirth & Niu, et.al, PRL (2002); Fang, et.al, Science (2003); Y. Yao & Niu, et.al. PRL (2004)]

	Analogies	
Berry curvature		Magnetic field
$\vec{\Omega}(\vec{k})$		$\vec{B}(\vec{r})$
Berry connection		Vector potential
$\vec{A}(\vec{k}) = \langle \psi i \frac{\partial}{\partial \mathbf{k}} \psi \rangle$		$\vec{A}(\vec{r})$
Berry phase		Aharonov-Bohm phase
$\oint d\vec{k} \cdot \vec{A}(\vec{k}) = \iint d^2k \Omega_z(\vec{k})$		$\oint d\vec{r} \cdot \vec{A}(\vec{r}) = \iint d^2r B_z(\vec{r})$
Chern number		Dirac monopole
$\iint d^2k \Omega_z(\vec{k}) = \text{integer}$		$\iint d^2r B_z(\vec{r}) = \text{integer } h/e$

Observable:
 Anomalous Hall effect

Anomalous hall conductivity

Two qualitatively different microscopic mechanisms:

$$\sigma_{xy}^{AH} = \sigma_{xy}^{AH,extrinsic} + \sigma_{xy}^{AH,intrinsic} \sim \int_{BZ} \frac{d^3\mathbf{k}}{(2\pi)^3} f_n(\mathbf{k}) \Omega_{n,z}(\mathbf{k})$$

Scattering effects

Connected to the Berry curvature

Linked to topological properties
of the Bloch states

Berry curvature is enhanced at the Weyl nodes

$\sigma_{xy}^{AH,intrinsic}$ depends only on the band structure

Y. Fang et. al., Science 302, 92 (2003).

F.D.M. Haldane et. al., Phys. Rev. Lett. 93, 206602 (2004).

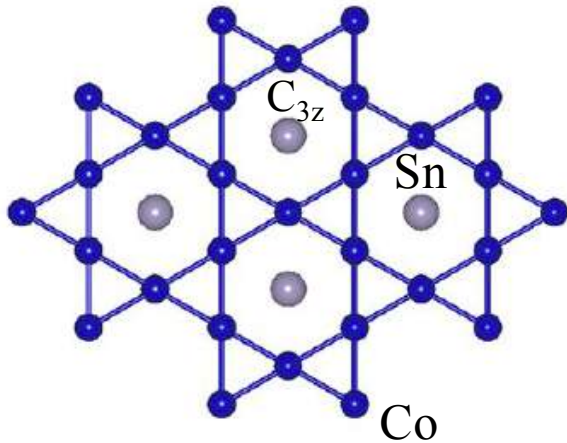
N. Nagaosa et. al., Rev. Mod. Phys. 82, 1539 (2010).

D. Xiao et. al., Rev. Mod. Phys. 82, 1959 (2010).

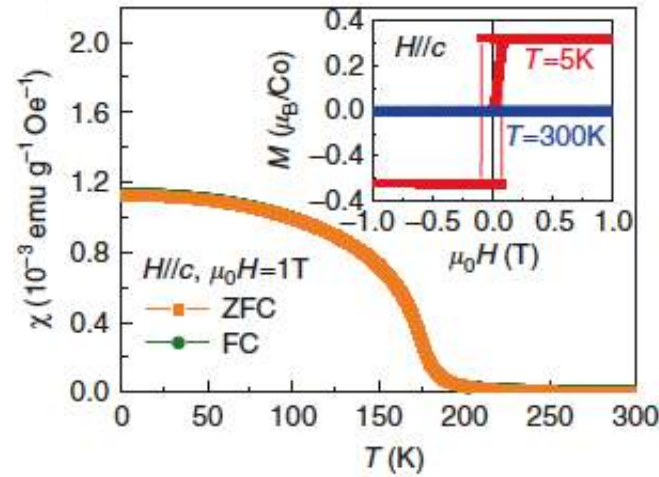
S. Nakatsuji et. al., Nature 527, 212 (2015).

Kagome ferromagnet $\text{Co}_3\text{Sn}_2\text{S}_2$: Predicted Weyl semimetal

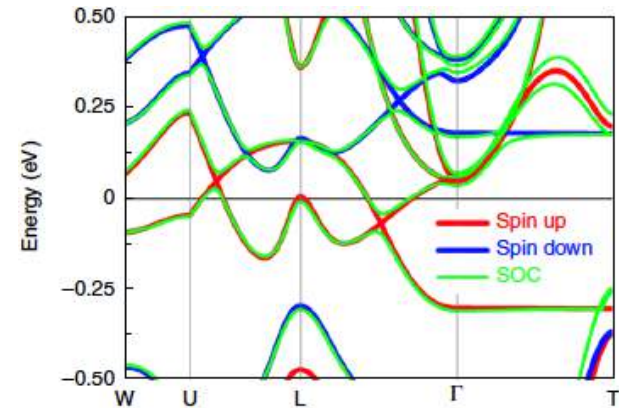
Kagome



Ferromagnetism

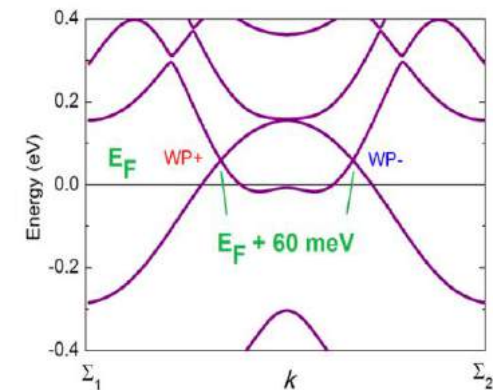
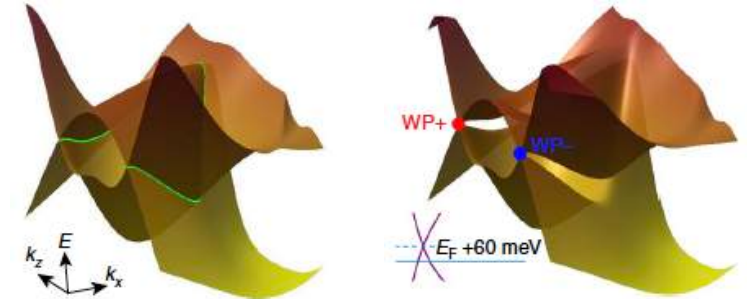
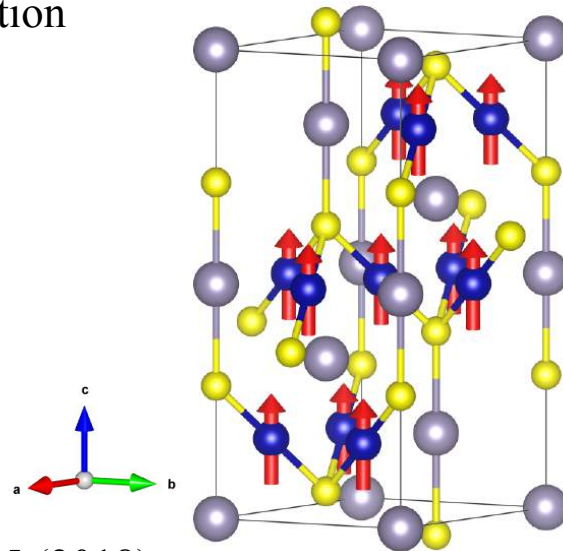


Weyl fermions



Kagome lattice with a C_{3z} -rotation

- Flat bands
- Dirac fermions
- Spin liquid phases

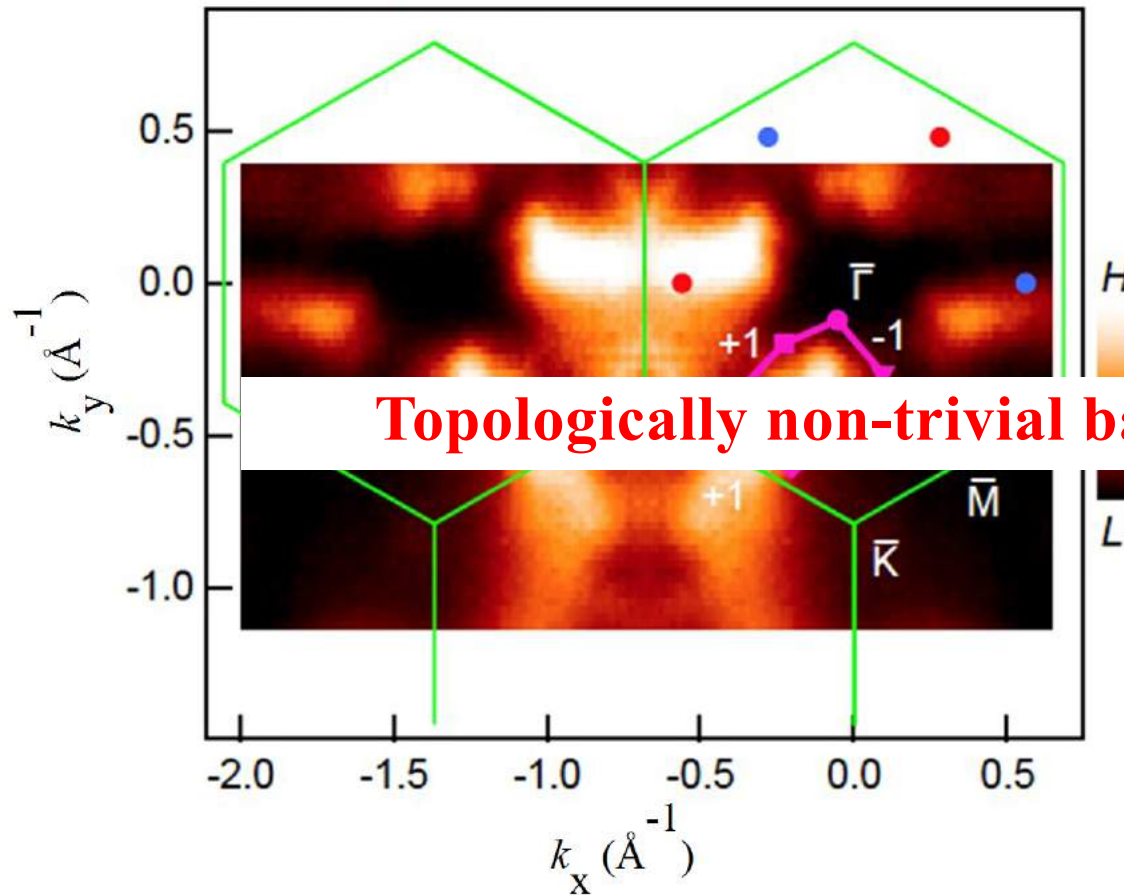


E. Liu et. al., Nat. Phys. 14, 1125 (2018).

Q. Wang et. al., Nat. Comm. 9, 3681 (2018).

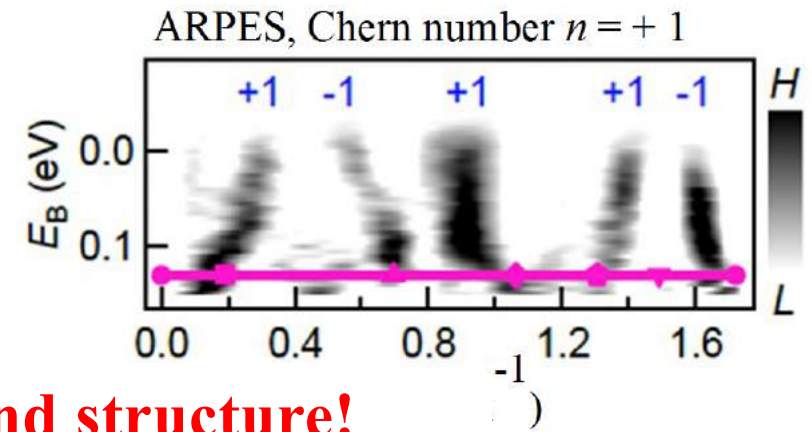
Topological ground state of $\text{Co}_3\text{Sn}_2\text{S}_2$ by ARPES

ARPES, $E_F \pm 5\text{meV}$ Fermi surface at $T = 22\text{ K}$

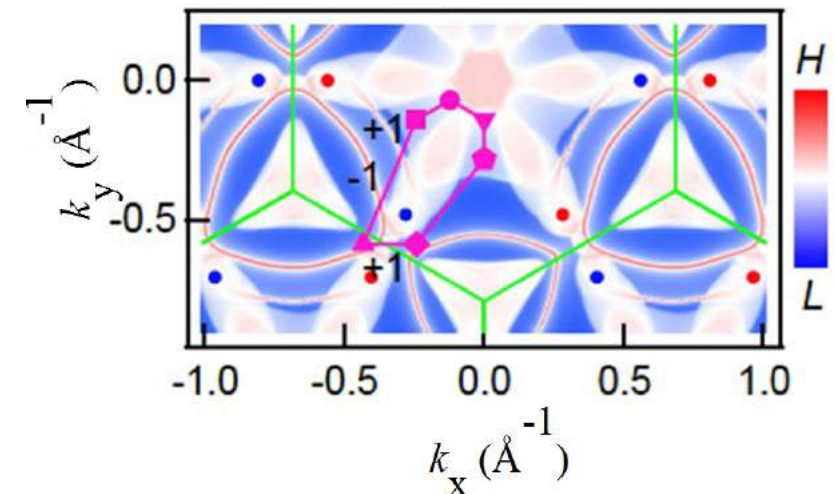


Topologically non-trivial band structure!

Energy-momentum cut along the purple loop



Calculated surface density of states at E_F



➤ Five crossings at the Fermi level.

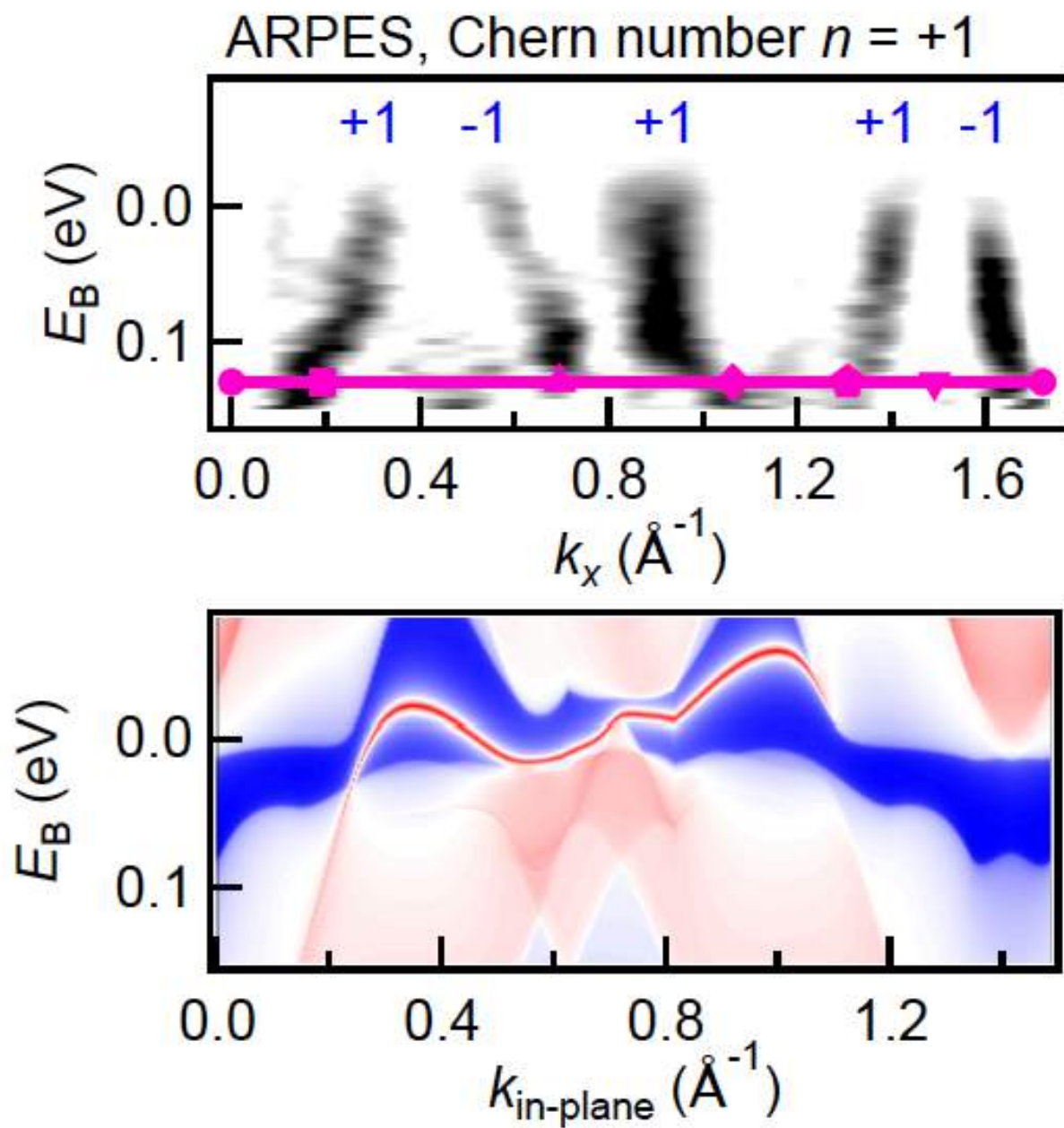
Inconsistent with any conventional surface state band structure.

➤ Loop encloses a Chern number of $n = +1$.

Weyl fermion lies inside the loop.

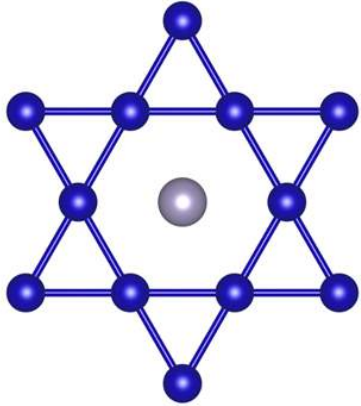
➤ One Weyl point, obtained from DFT, projects inside our closed loop.

For reference: side-by-side comparison of the loop cut, ARPES & DFT

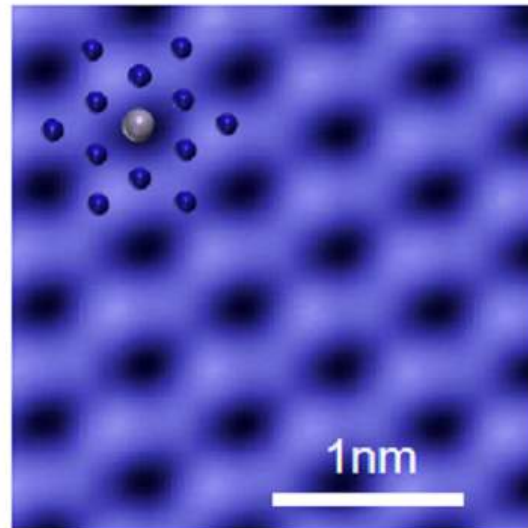


Topographic image of the CoSn surface

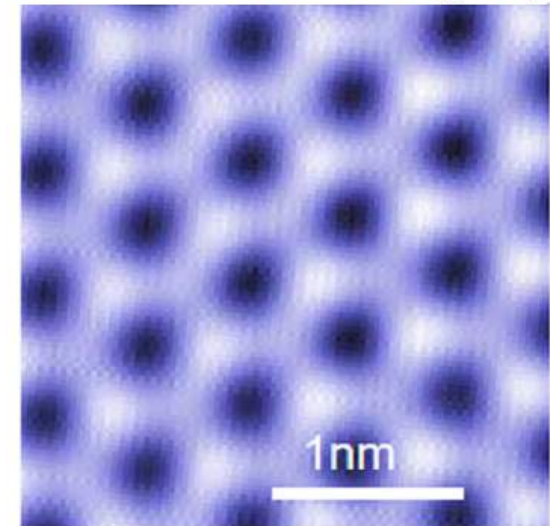
Co₃Sn kagome lattice



CoSn surface



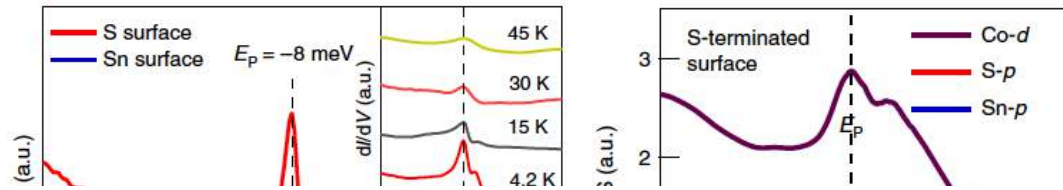
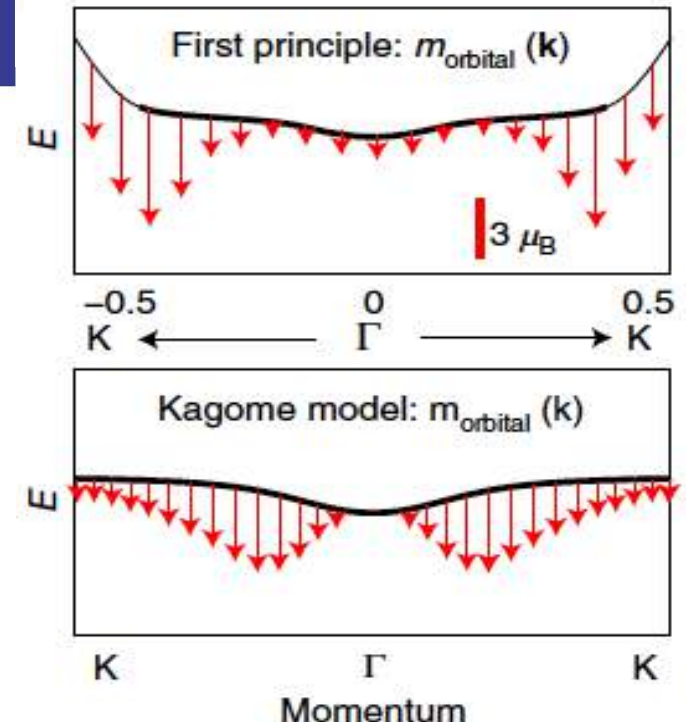
FeSn surface in Fe₃Sn₂



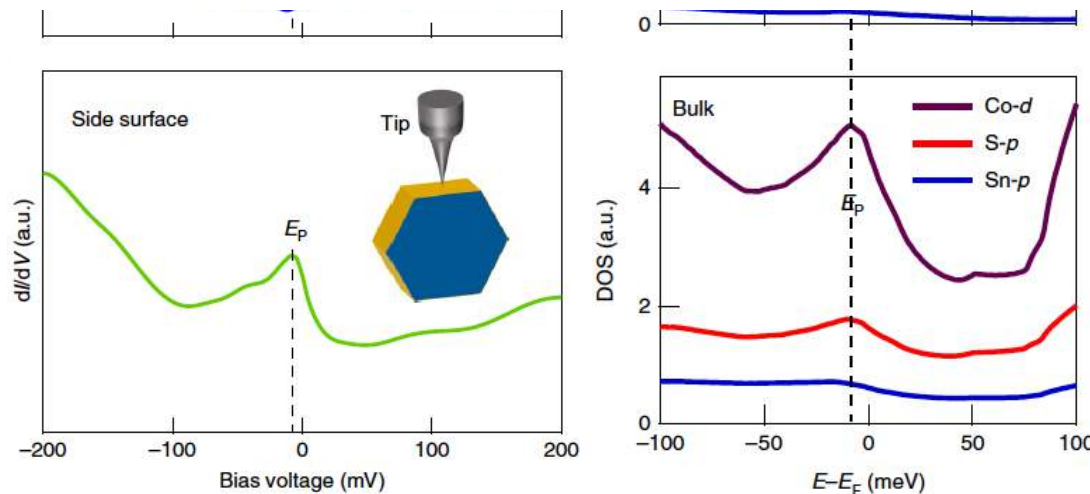
Consistent with the transition metal based kagome lattice structure!

Negative flat band magnetism in a spin-orbit-coupled correlated kagome magnet

Jia-Xin Yin^{1,12}, Songtian S. Zhang^{1,12}, Guoqing Chang^{1,12}, Qi Wang², Stepan S. Tsirkin³, Zurab Guguchia^{1,4}, Biao Lian⁵, Huibin Zhou^{6,7}, Kun Jiang⁸, Ilya Belopolski¹, Nana Shumiya¹, Daniel Multer¹, Maksim Litskevich¹, Tyler A. Cochran¹, Hsin Lin⁹, Ziqiang Wang⁸, Titus Neupert³, Shuang Jia^{6,7}, Hechang Lei² and M. Zahid Hasan^{1,10,11*}



Topological point, line nodes and flat band concentrate the Berry curvature and is expected to boost anomalous hall response!

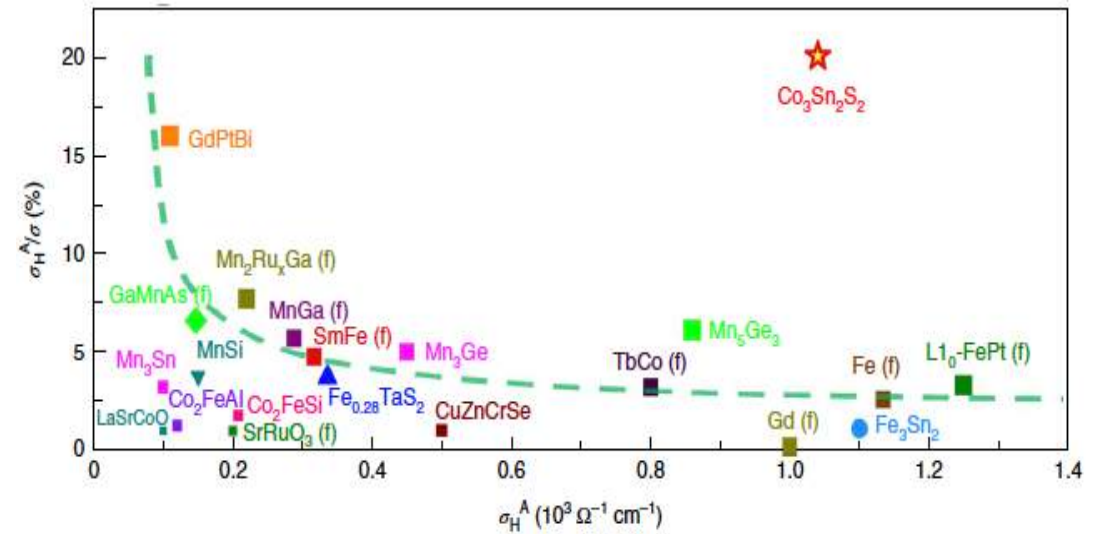
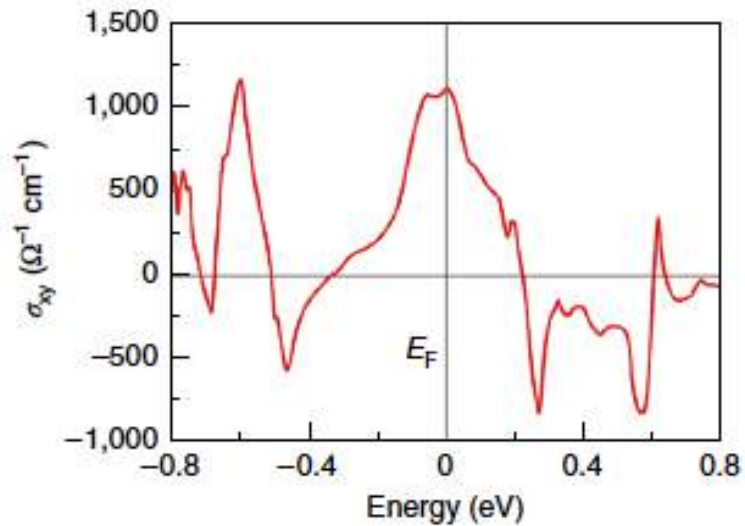
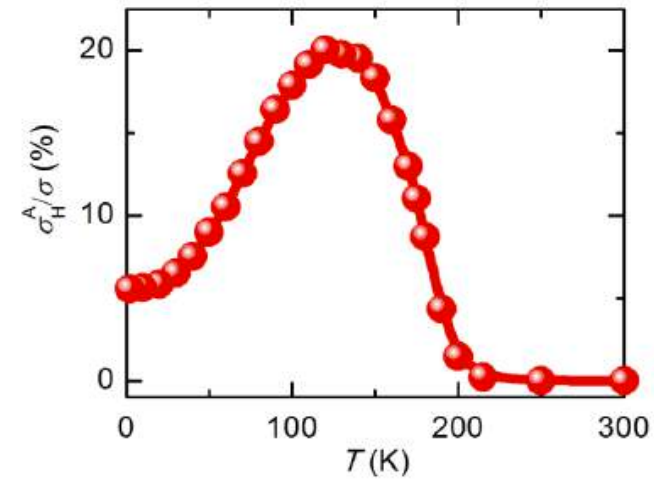
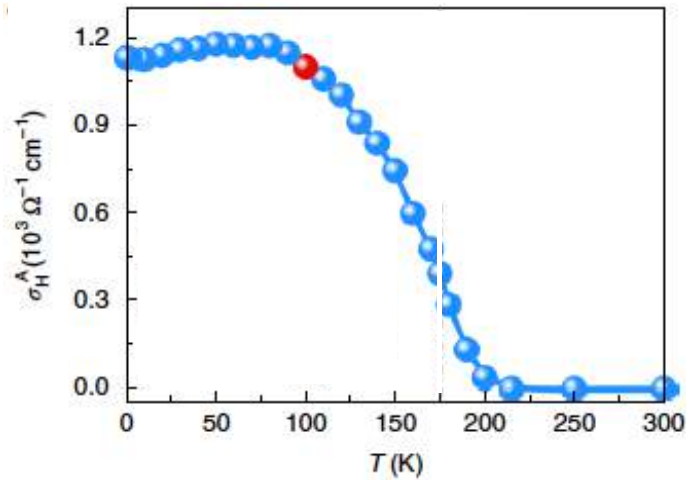


➤ Strong diamagnetism associated with flat band.

$$m_{\text{orbital}}(\mathbf{k}) \approx -\frac{\mathbf{k}^2 t^2 \lambda}{k^4 t^2 + 48 \lambda^2}$$

➤ The flat band with strong Berry curvature effects.

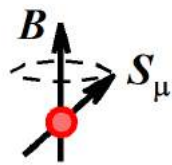
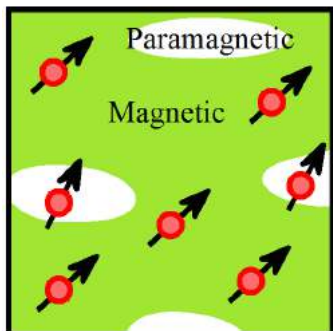
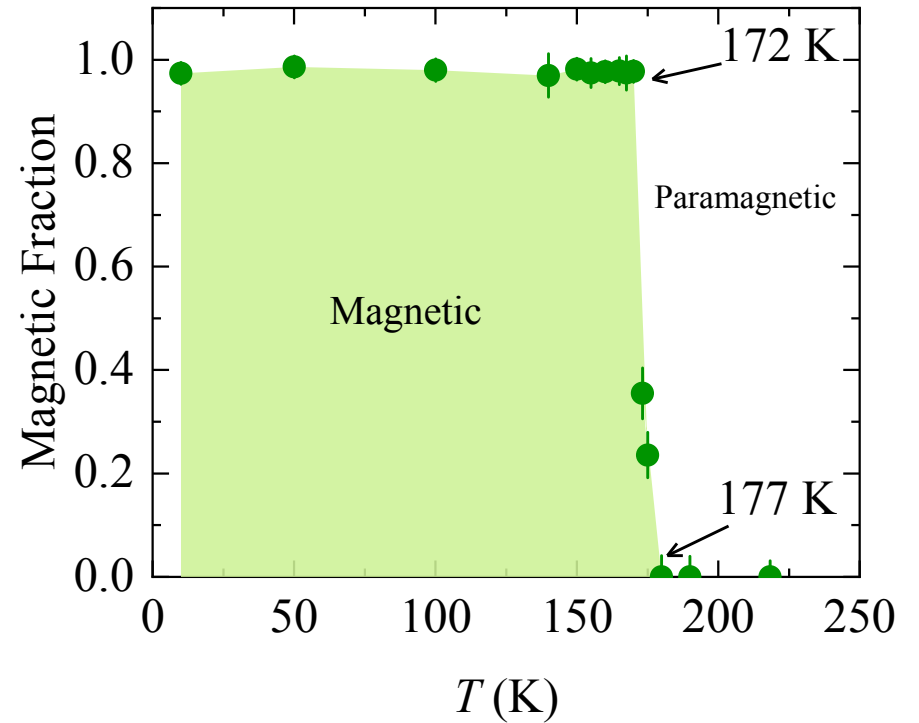
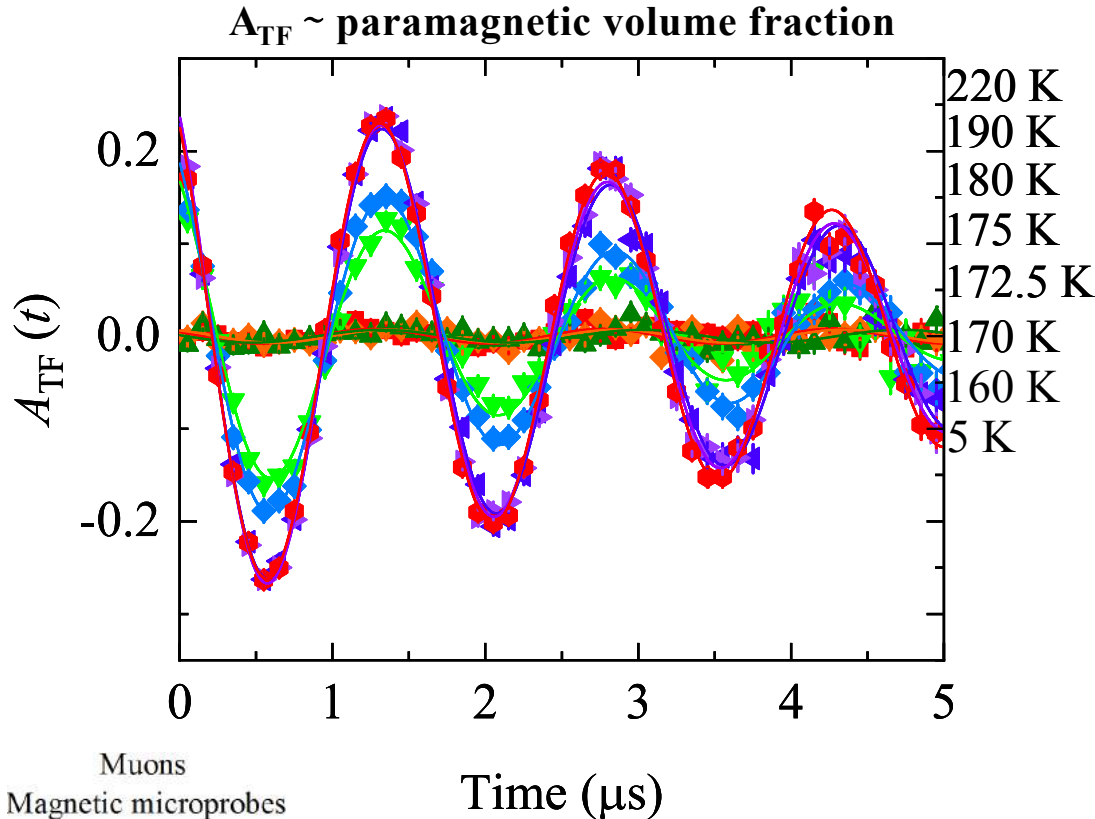
Anomalous Hall Conductivity and anomalous Hall angle



$\text{Co}_3\text{Sn}_2\text{S}_2$ is the first material hosting both a large AHC and a giant AHA.

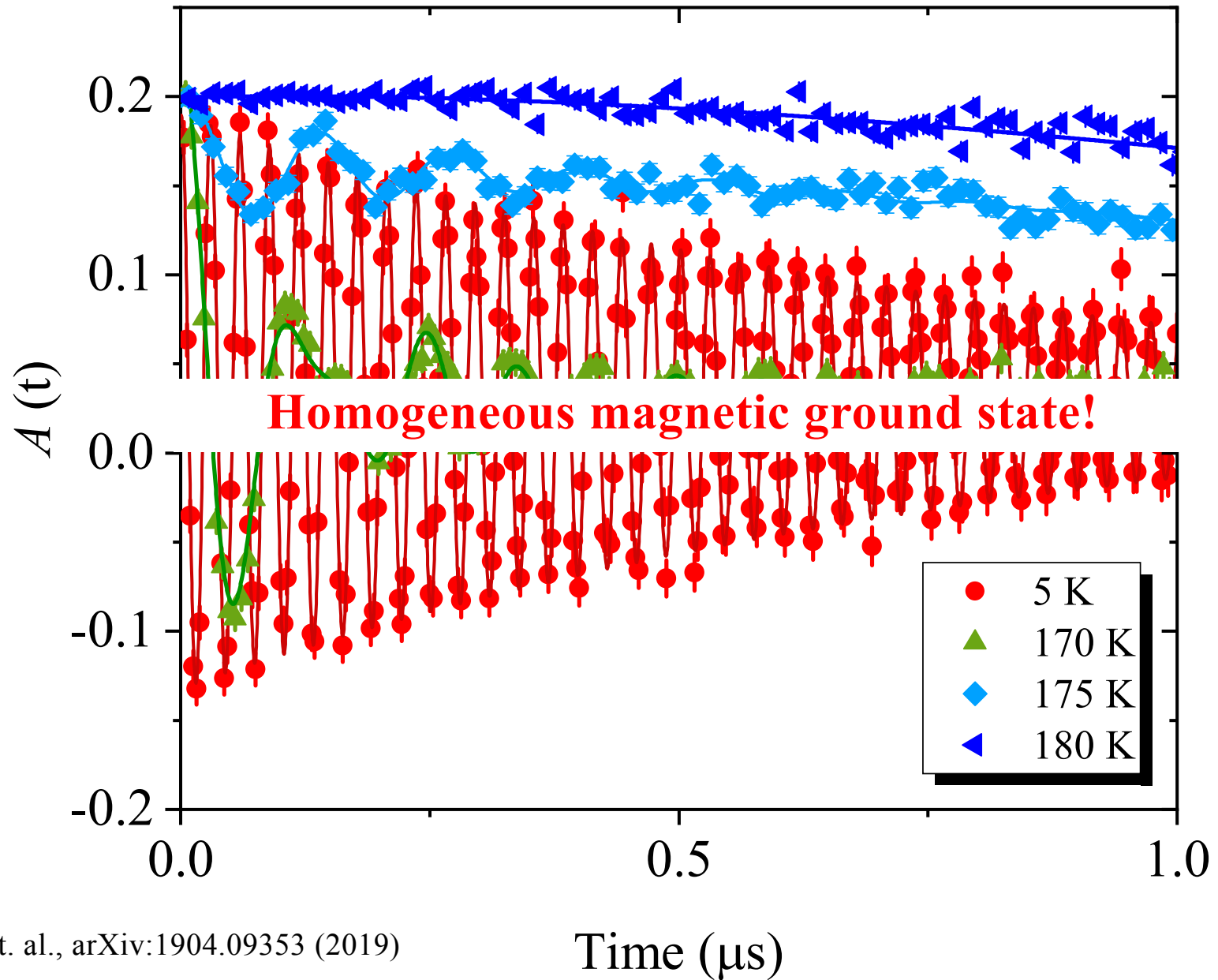
AHE physics connected to intrinsic band Berry curvature.

Temperature dependence of the total magnetic fraction in $\text{Co}_3\text{Sn}_2\text{S}_2$
Muon Spin Rotation

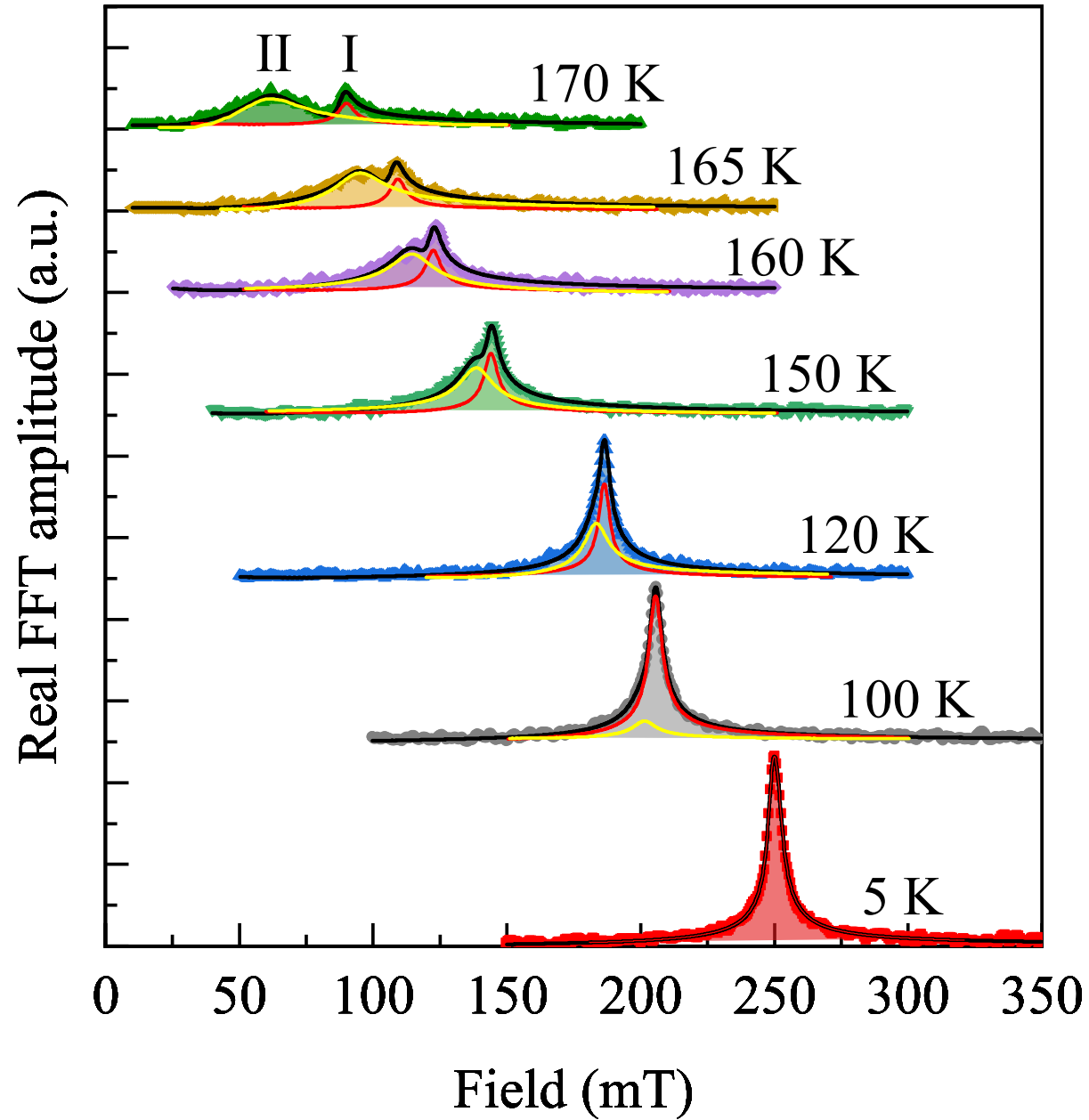


100 % of the sample volume is magnetic!
Phase separation between magnetic and paramagnetic regions in the narrow temperature range!

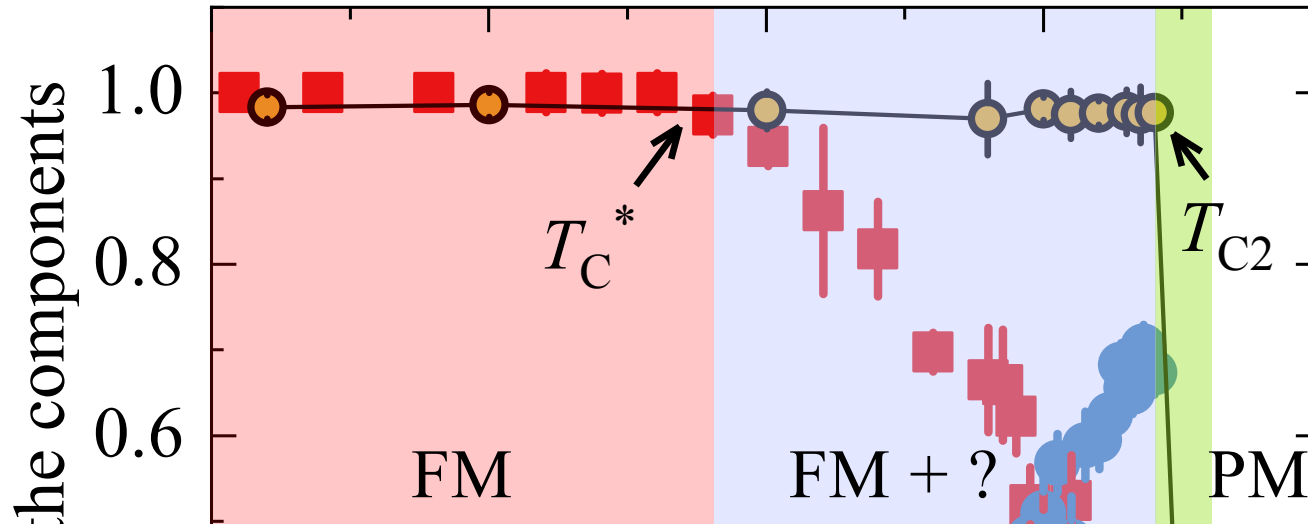
Muon-spin precession in internal magnetic field of $\text{Co}_3\text{Sn}_2\text{S}_2$



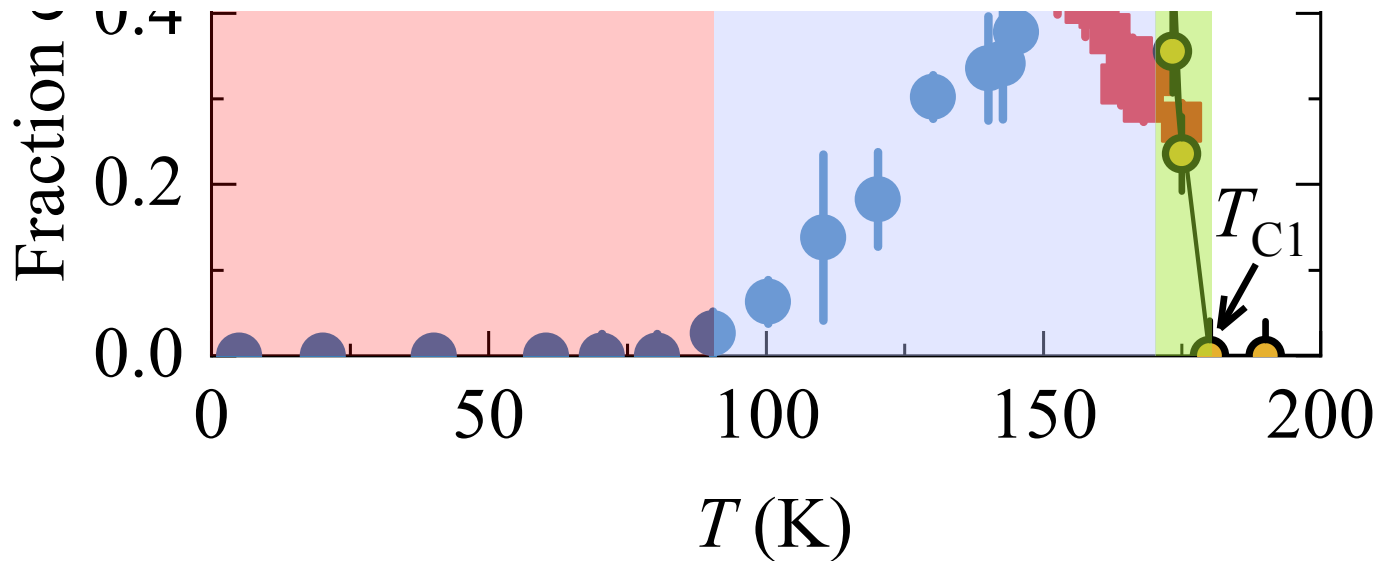
Fourier transform amplitude at various temperatures for $\text{Co}_3\text{Sn}_2\text{S}_2$



The temperature dependence of the magnetic fractions in $\text{Co}_3\text{Sn}_2\text{S}_2$



The presence of two distinct magnetically ordered regions in $\text{Co}_3\text{Sn}_2\text{S}_2$!

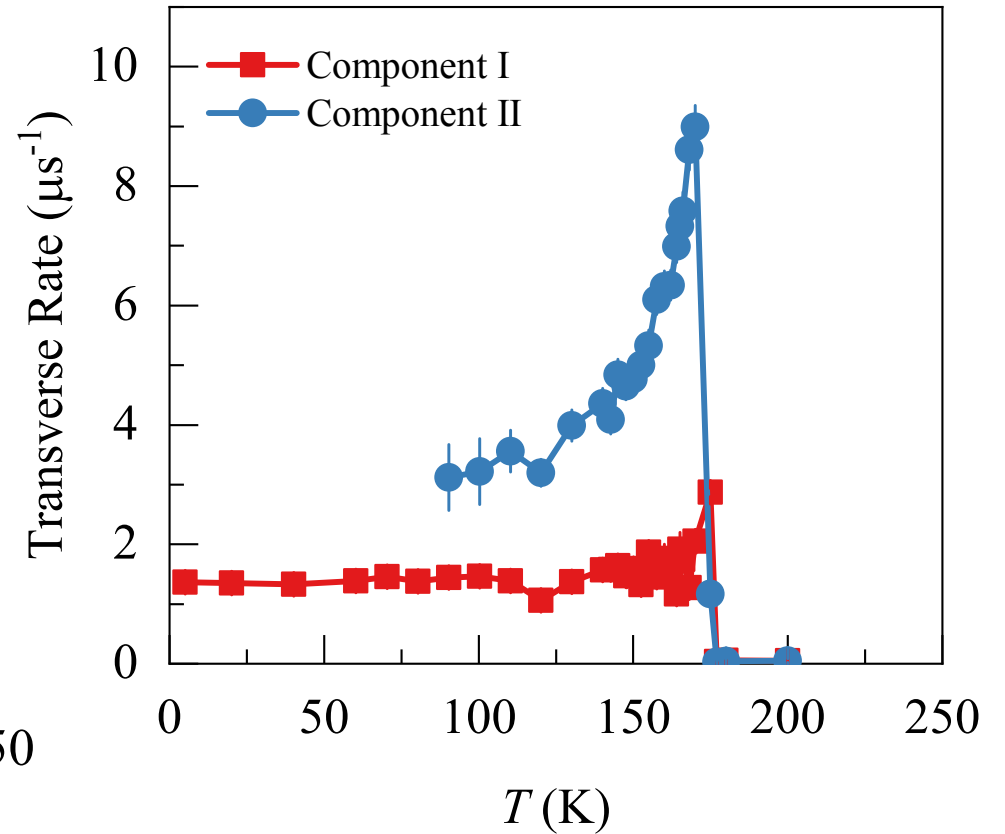
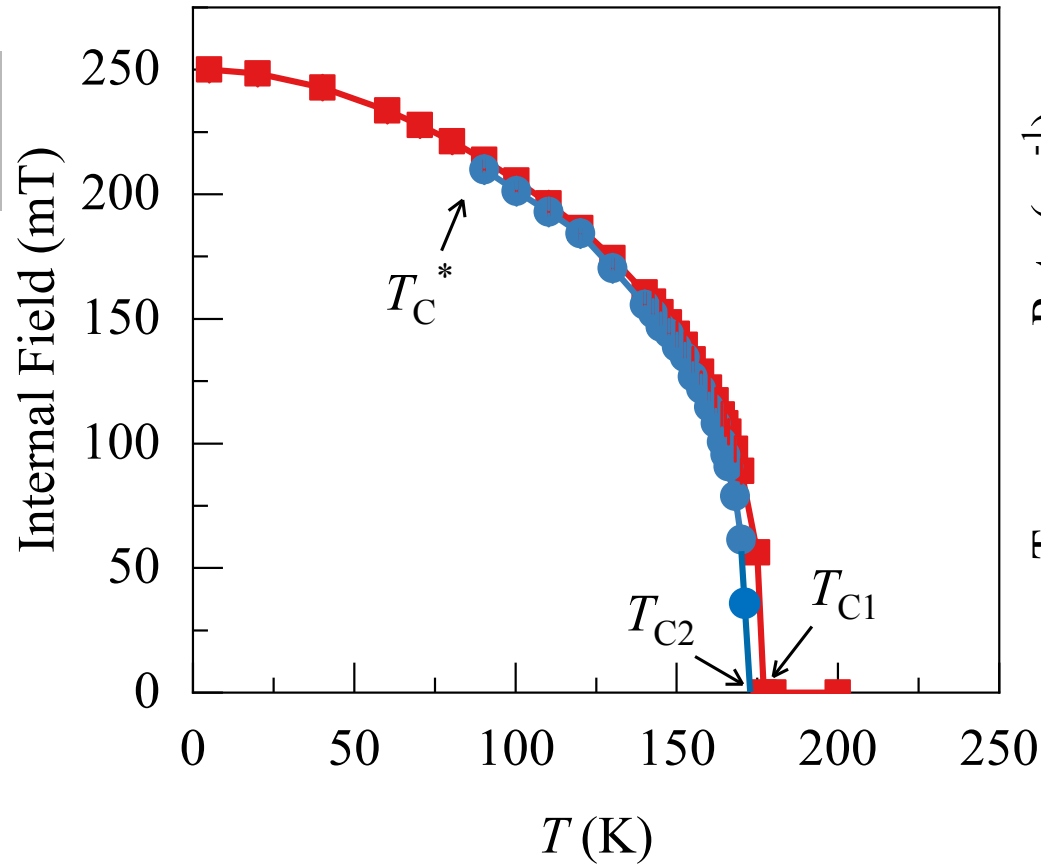


Ferromagnetic
 $T < T_C^*$

Phase separation between FM and novel magnetic state
 $T_C^* < T < T_{C2}$

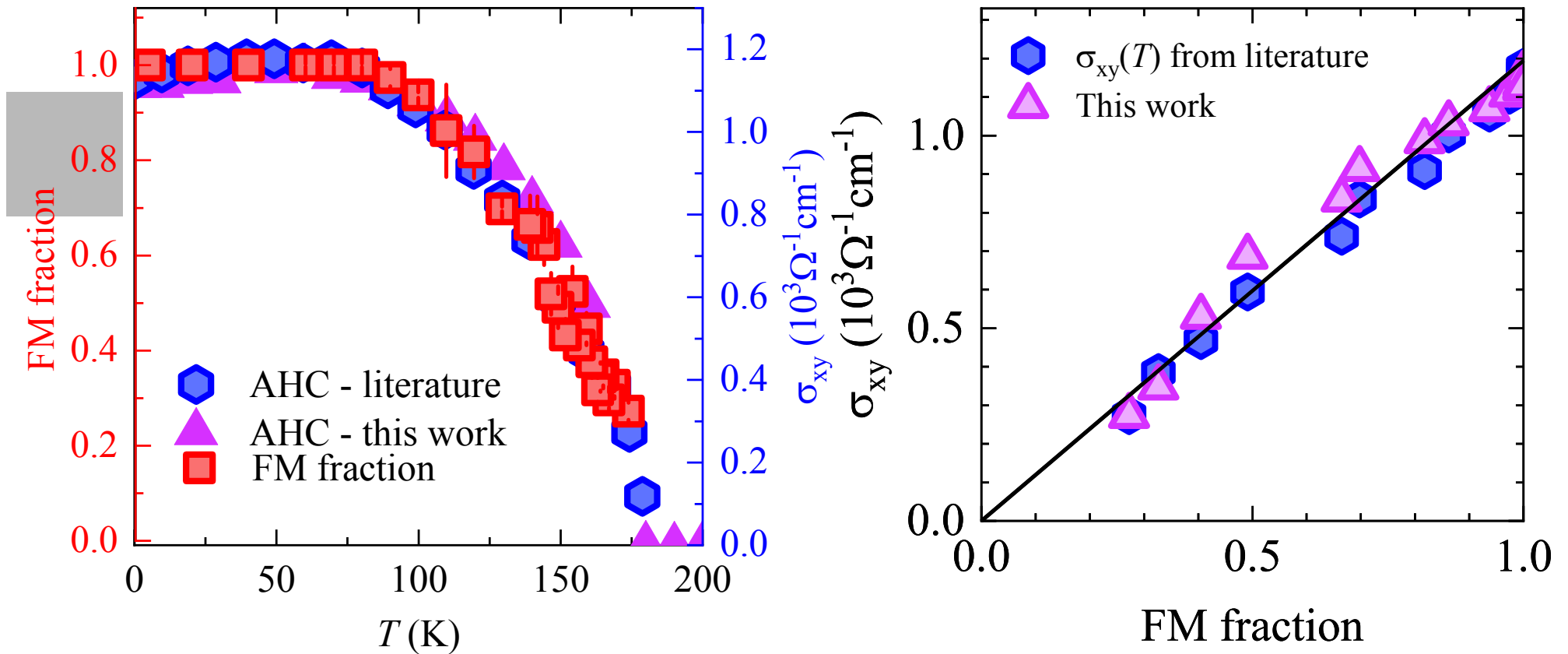
FM state with low volume
 $T_{C2} < T < T_{C1}$

Internal field ~ ordered moment



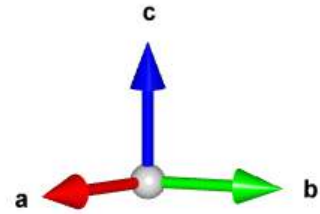
- **Two components have slightly different transition temperatures: $T_{C1} \approx 177$ K, $T_{C2} \approx 172$ K.**
- **Novel magnetic state gives broader internal field distribution.**

Scaling between FM fraction and anomalous hall conductivity

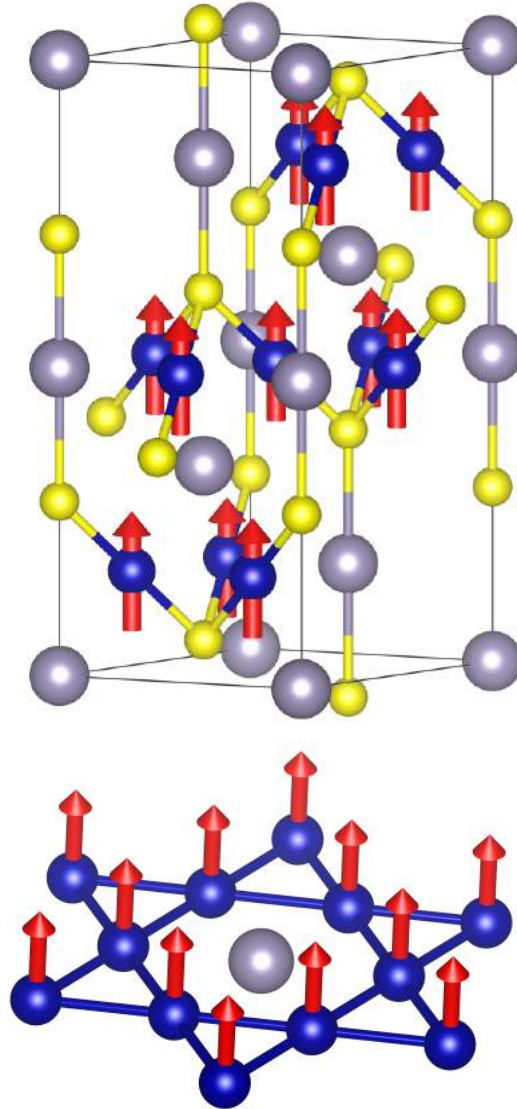


- Striking correlation between AHC and FM volume fraction.
- Novel magnetic state suppresses AHC.
- Magnetic competition drives thermal evolution of anomalous Hall conductivity.

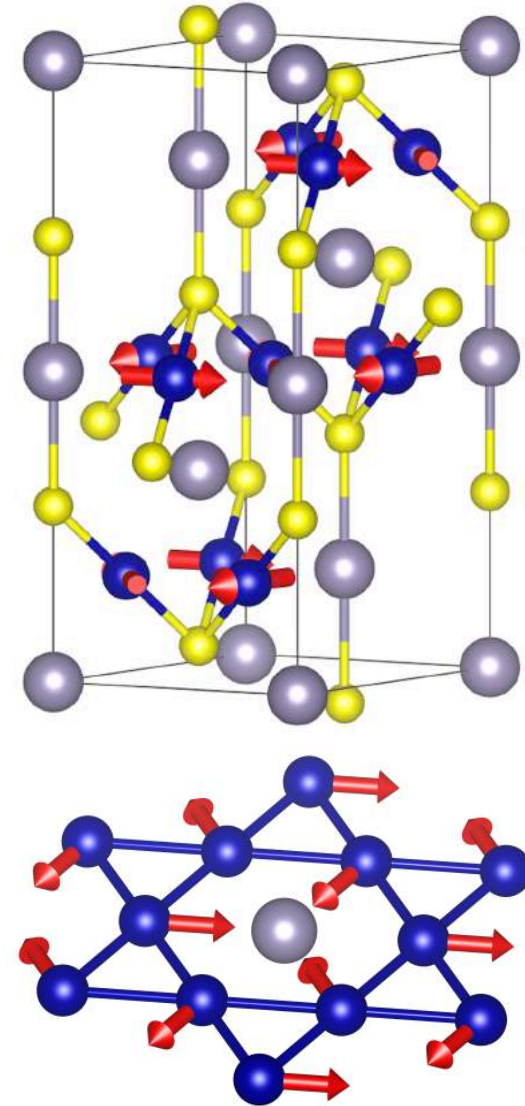
Possible Magnetic Structures in $\text{Co}_3\text{Sn}_2\text{S}_2$



$R-3m' (0, 0, m_z)$



$R-3m (m_x, 0, 0)$

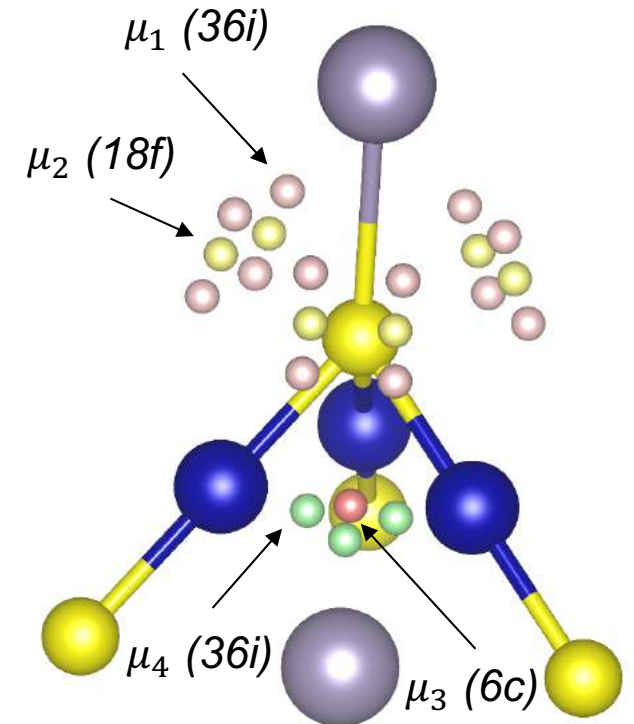


Lowest energy configuration according to DFT: FM with the moments along the c-axis.
The in-plane AFM configuration has a higher energy of 20 meV/Co atom, relative to FM order.

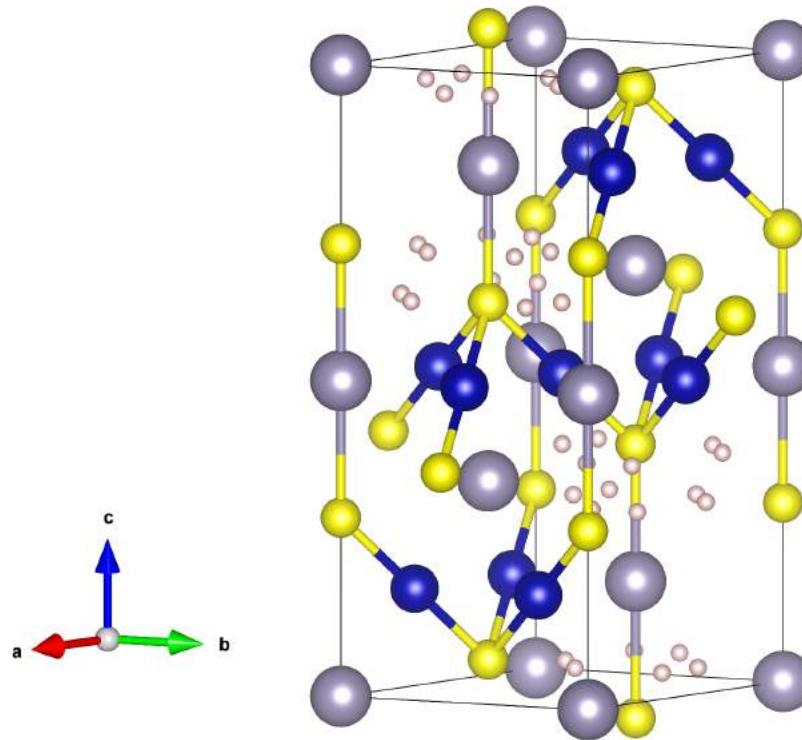
Candidate Muon Stopping Sites in $\text{Co}_3\text{Sn}_2\text{S}_2$

- Four sites identified in total

Site index	Position	Wyckoff position	$V - V_{max}$ (eV)
1	[0.24,0.296,0.372]	36i	0
2	[0.416,0,0]	18f	-0.114151807
3	[0,0,0.139]	6c	-1.76914892
4	[0.784,0.392,0.209]	36i	-2.367799634



- We can discount sites 2, 3 and 4 due to the large potential difference



- **Only one muon site at most general $36i$ position:**

$$r_{\mu} = [0.24, 0.296, 0.372]$$

- **In each of the considered structures (FM or AFM), muon site is magnetically equivalent.**

Internal field sensed by the muon has basically two contributions



➤ Dipolar field.

Due to localised electrons.

➤ Hyperfine contact field.

Due to the electron spin density at the muon site and originates from the itinerant electrons.

Hyperfine coupling constant was determined from the muon knight shift and macroscopic susceptibility measurements.

The field was calculated for each structure.

Internal field sensed by the muon has basically two origins

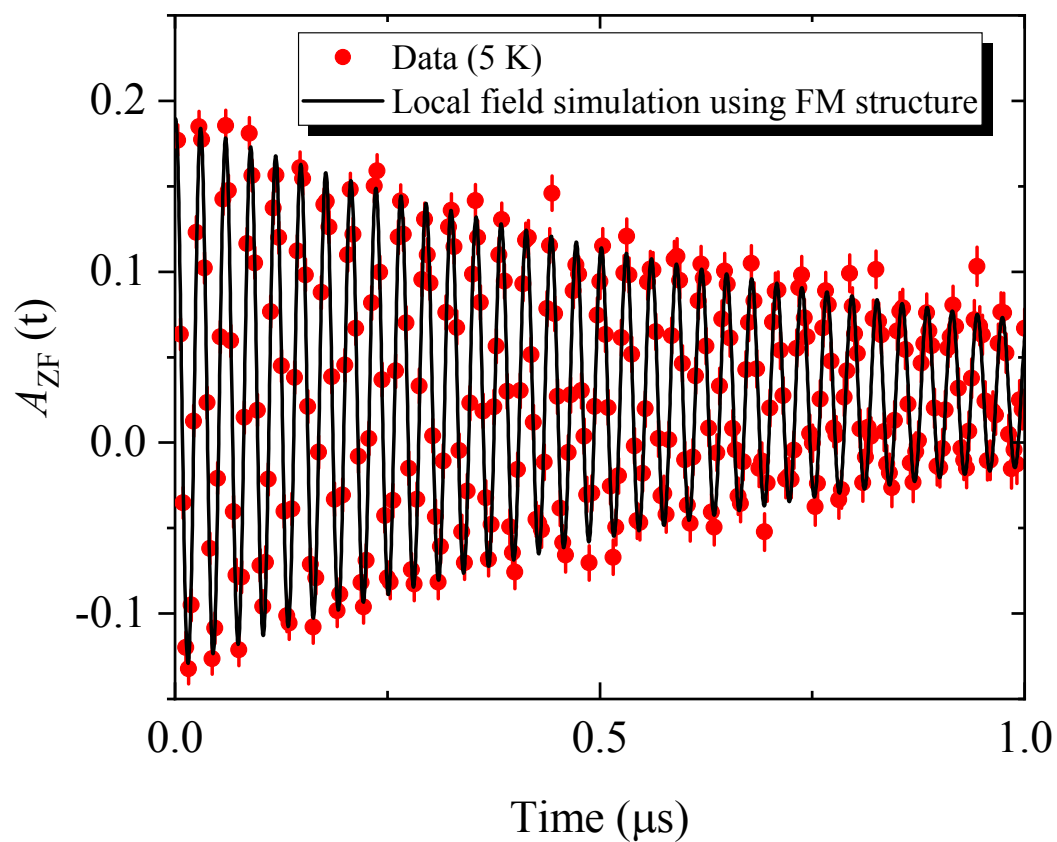
$$\mathbf{B}_\mu = \mathbf{B}_c + \mathbf{B}_{\text{dip}}$$

- Contact field $\propto e|\Psi(\mathbf{r}_\mu)|^2$
- Dipolar contribution

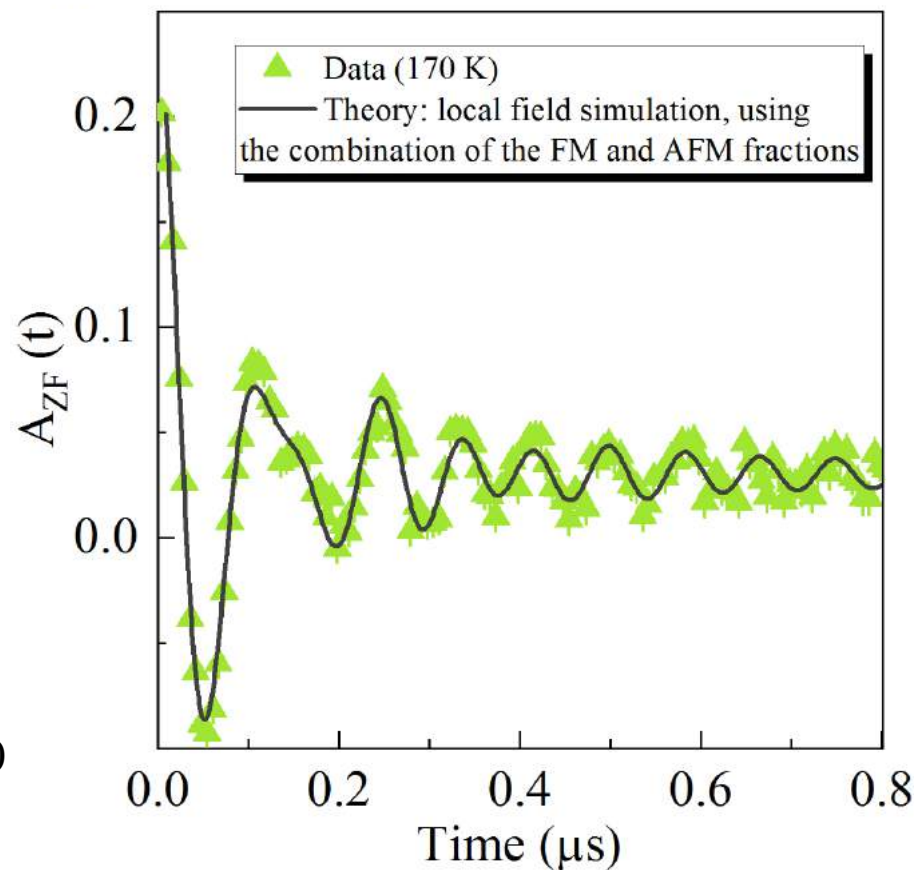
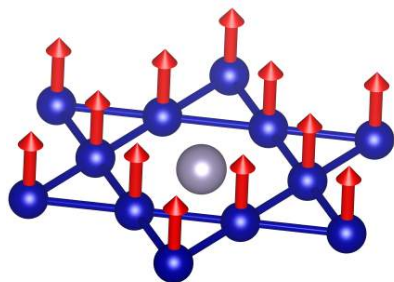
$$\mathbf{B}_{\text{dip}} = \frac{\mu_0}{4\pi} \sum_j \frac{1}{r_j^3} \left[\frac{(3\mathbf{m}_j \cdot \mathbf{r}_j)}{r_j^2} \mathbf{r}_j - \mathbf{m}_j \right]$$

$$B_{\text{dip}} \simeq \frac{\mu_0}{4\pi} \frac{m}{r^3}$$

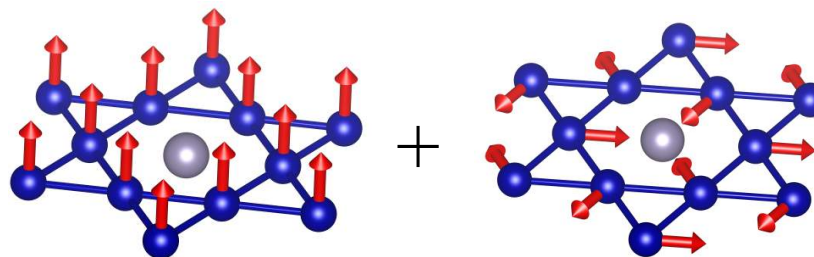
Local Field Simulation at the Muon Stopping Site in $\text{Co}_3\text{Sn}_2\text{S}_2$



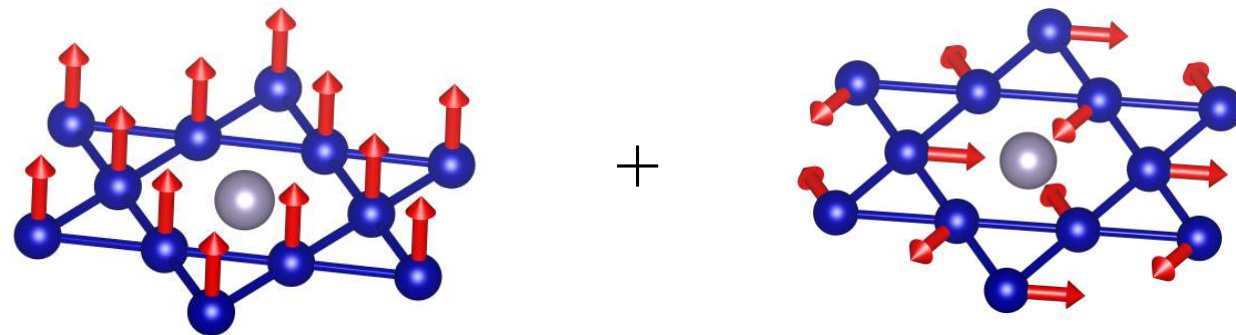
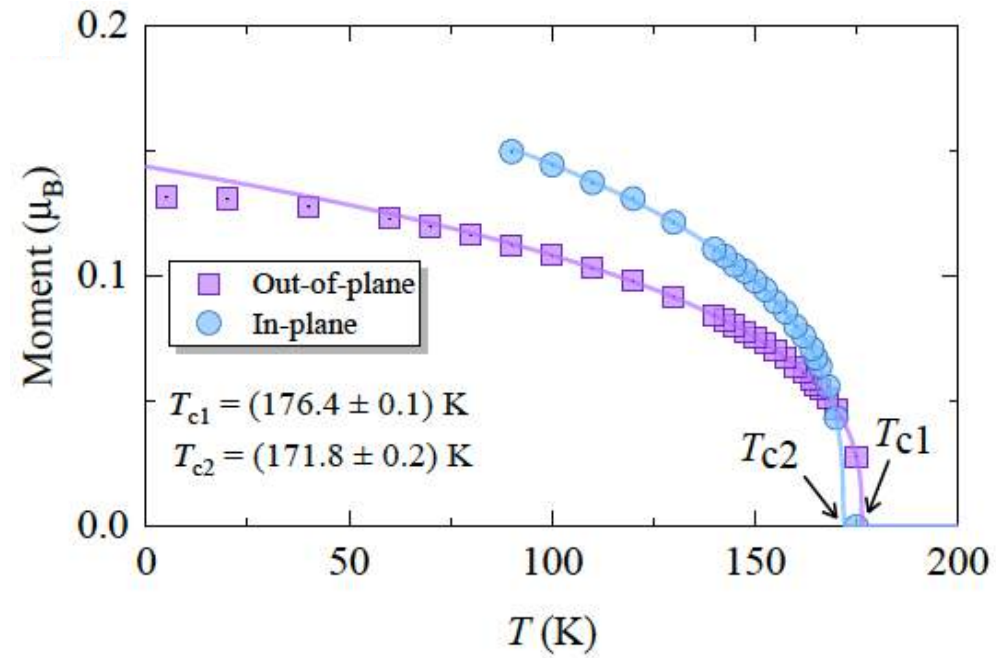
$$m_{\text{FM}} (5 \text{ K}) = 0.14 \mu_{\text{B}}$$



$$100 \text{ K} - m_{\text{FM}} = 0.11 \mu_{\text{B}} \quad m_{\text{AFM}} = 0.15 \mu_{\text{B}}$$

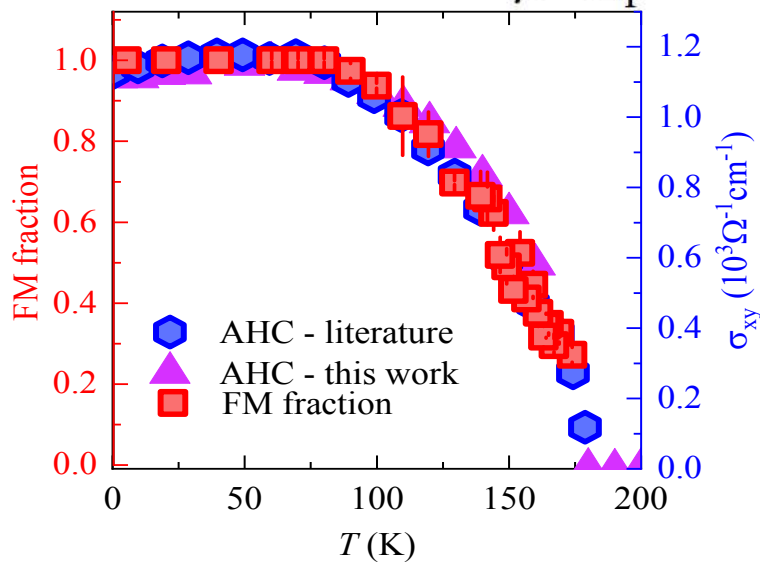
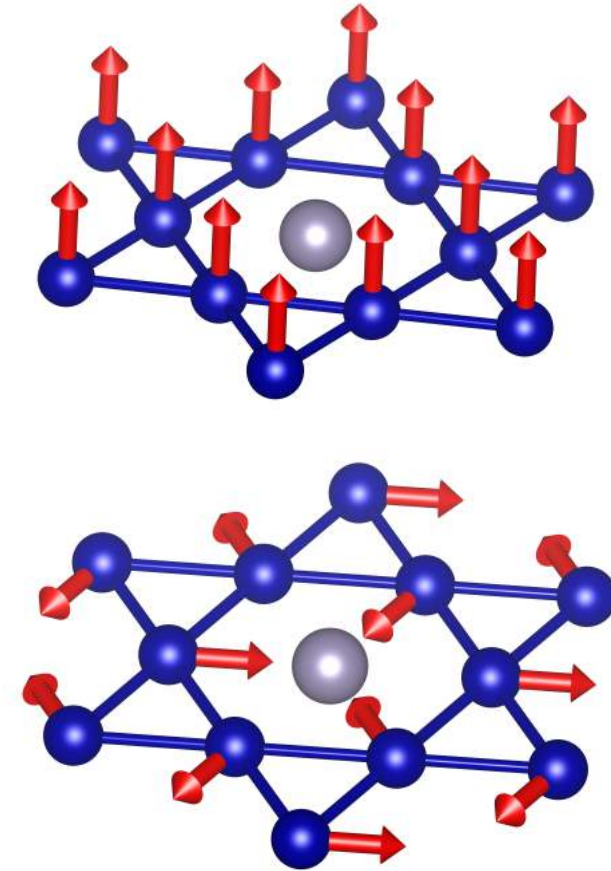
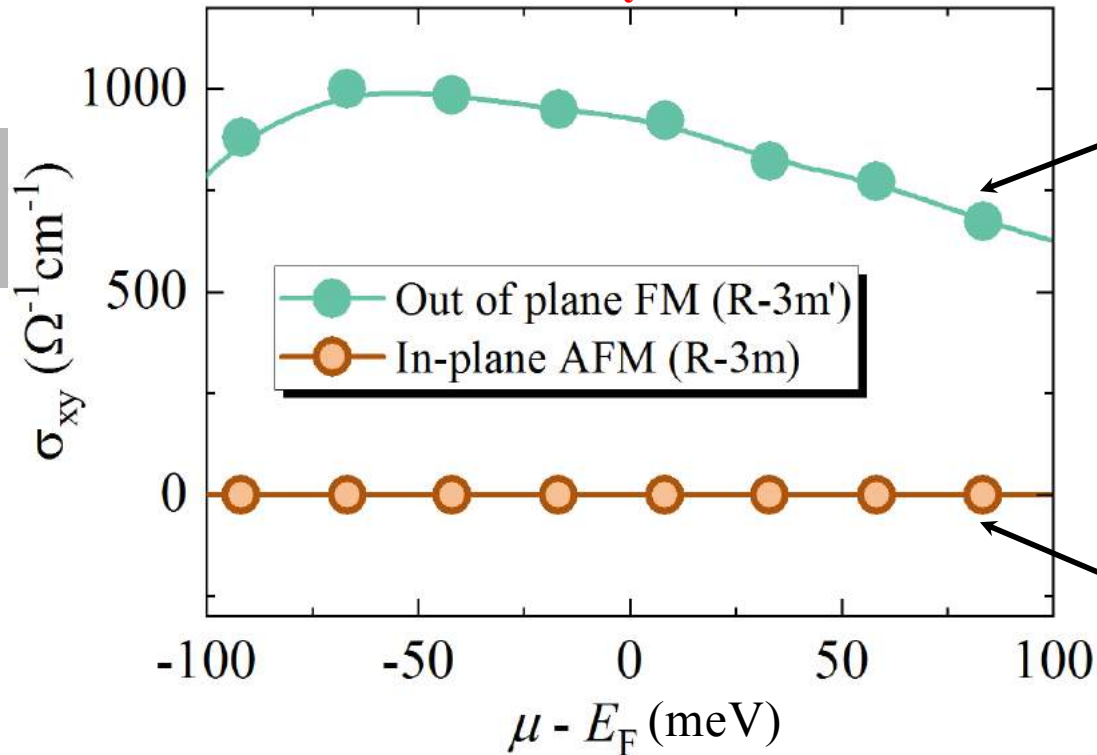


The temperature dependence of the magnetic moment in $\text{Co}_3\text{Sn}_2\text{S}_2$



Calculated In-plane anomalous Hall conductivity in $\text{Co}_3\text{Sn}_2\text{S}_2$

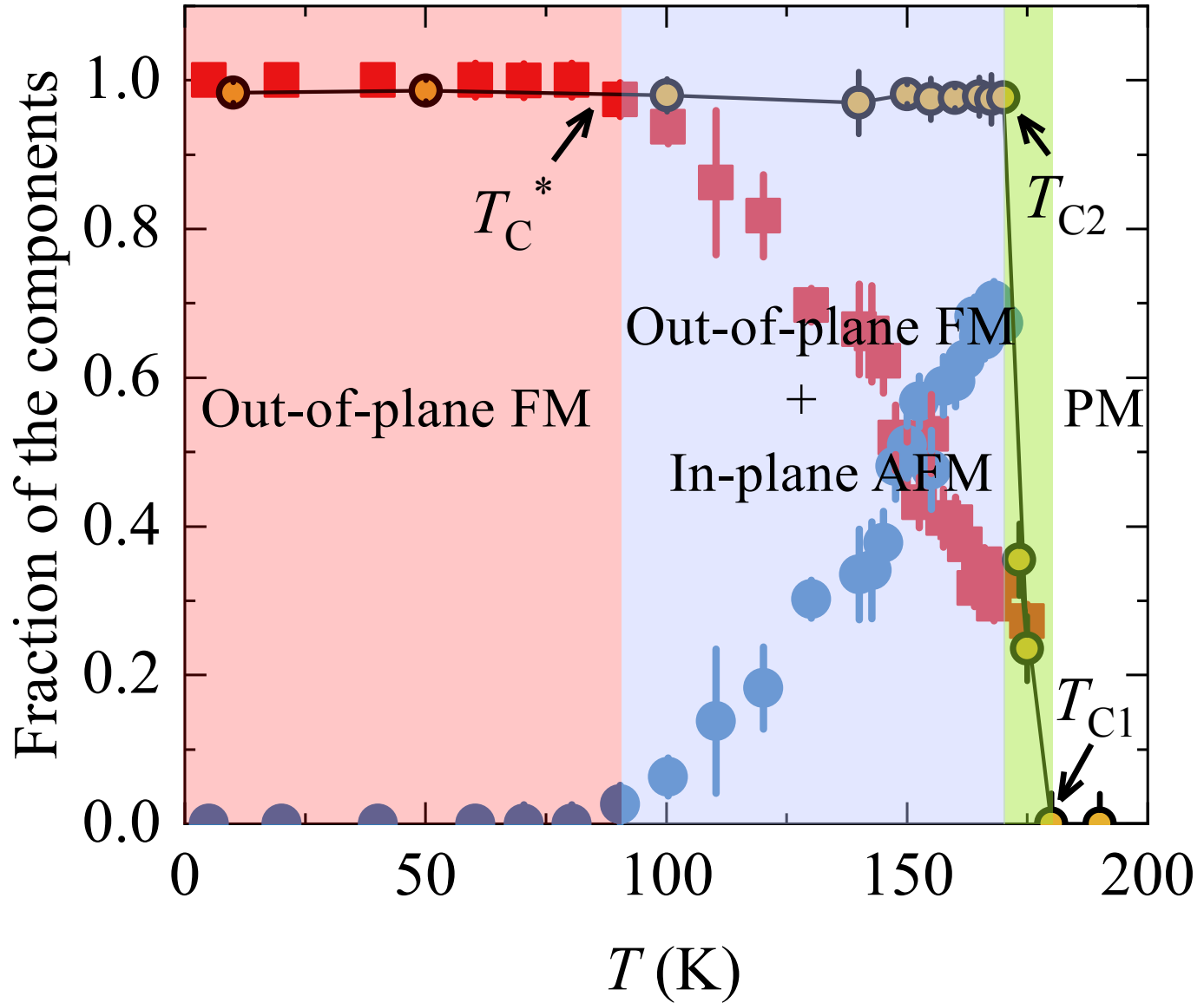
AHC is dominated by the FM structure!



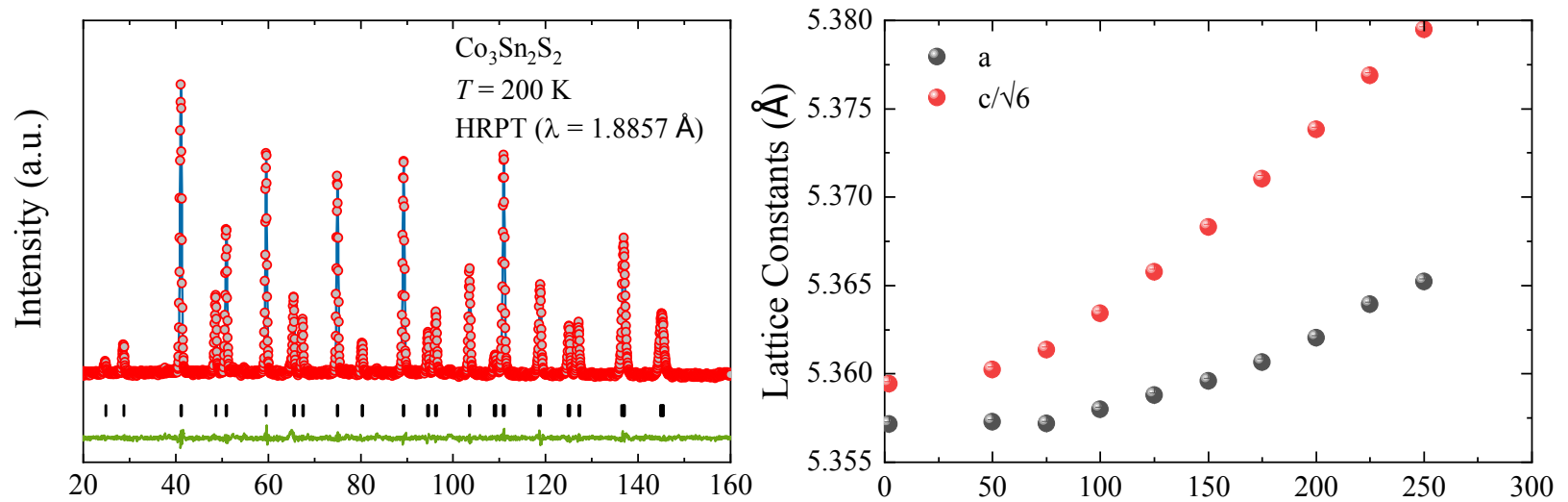
➤ **We can tune the competition between FM and AFM states and have control of the Berry curvature induced AHC by varying the temperature.**

➤ **Thermal tuning of Berry curvature!**

Schematic magnetic phase diagram as a function of temperature

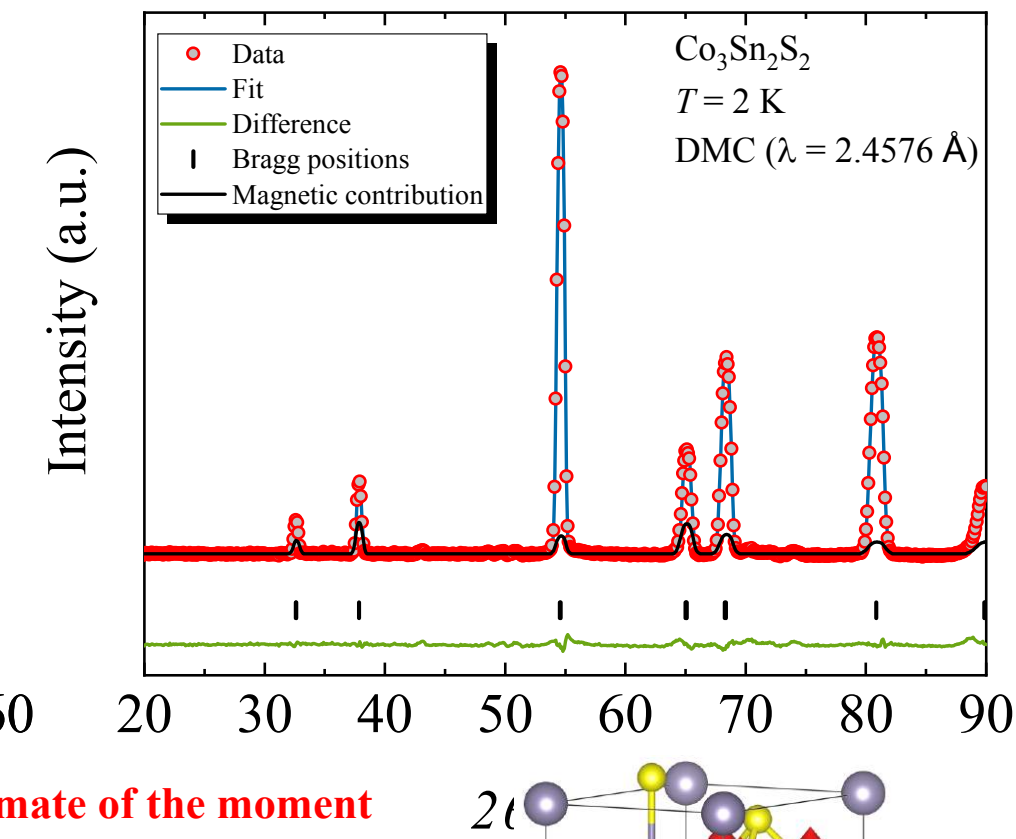
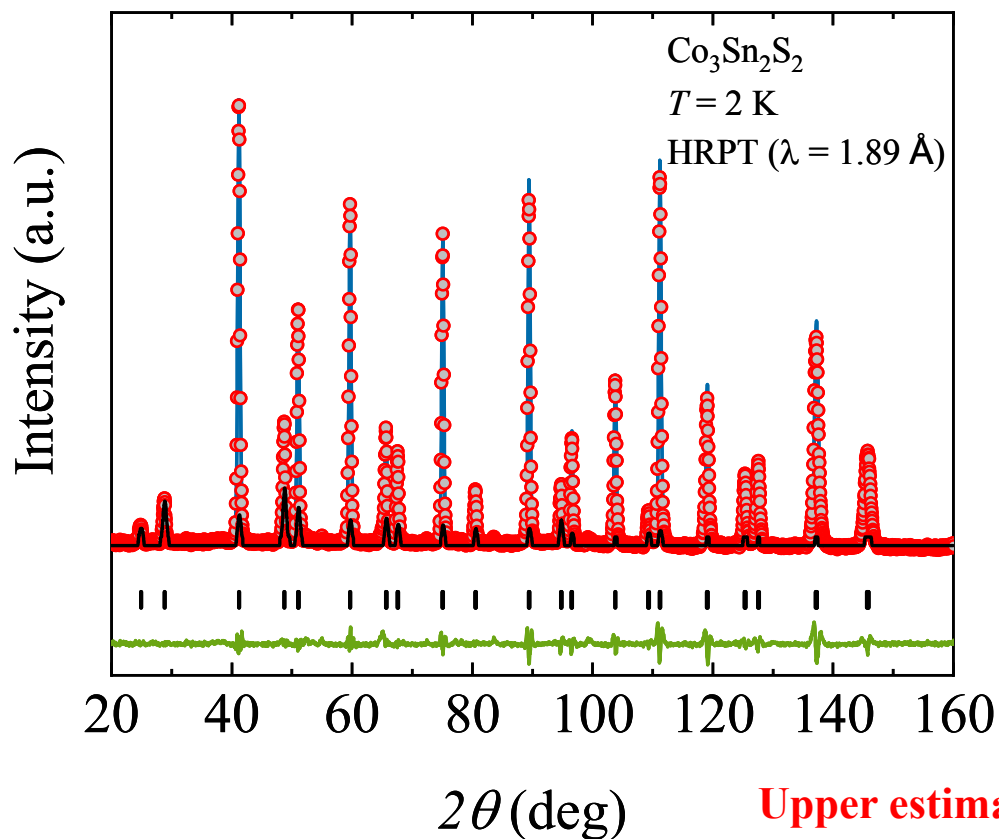


Neutron Diffraction on $\text{Co}_3\text{Sn}_2\text{S}_2$



Substantial coupling between the magnetic ordering and the crystal lattice!

Neutron Diffraction on $\text{Co}_3\text{Sn}_2\text{S}_2$

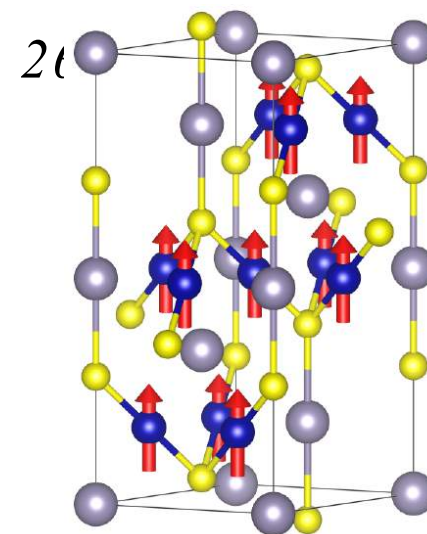


0.2 - 0.3 μ_B

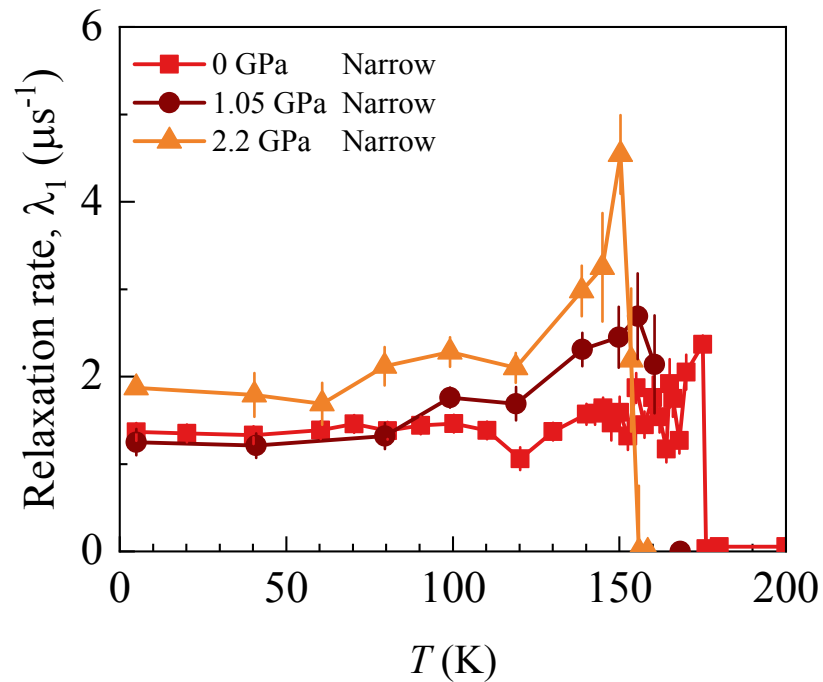
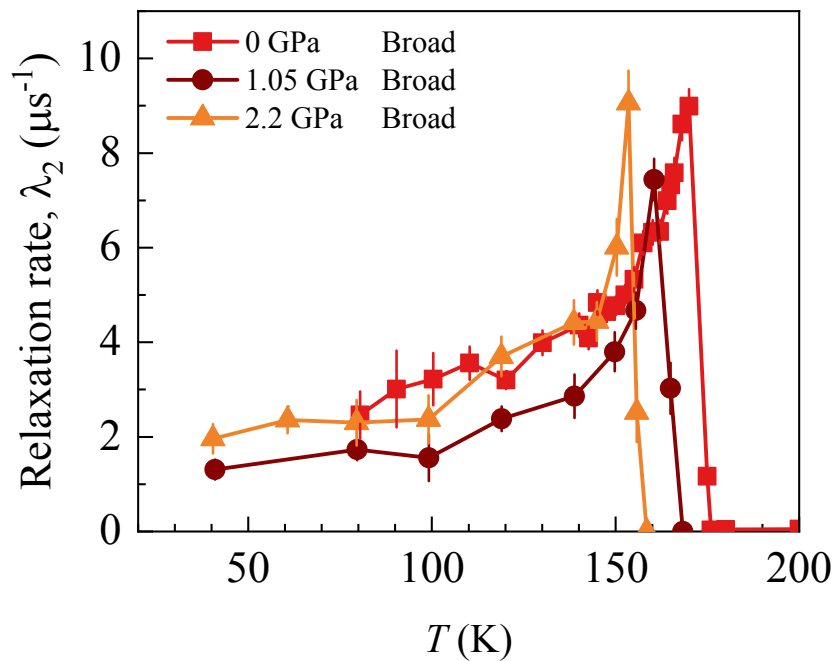
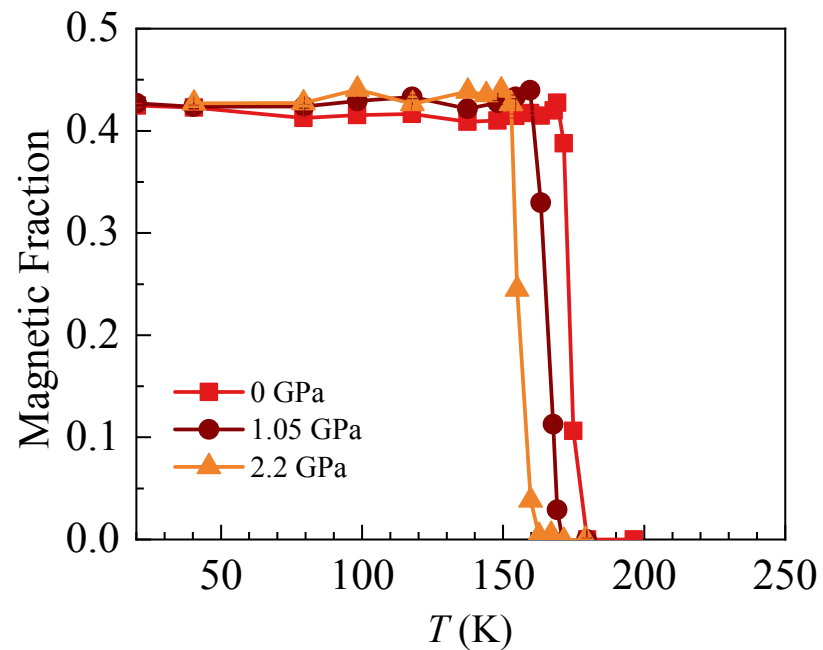
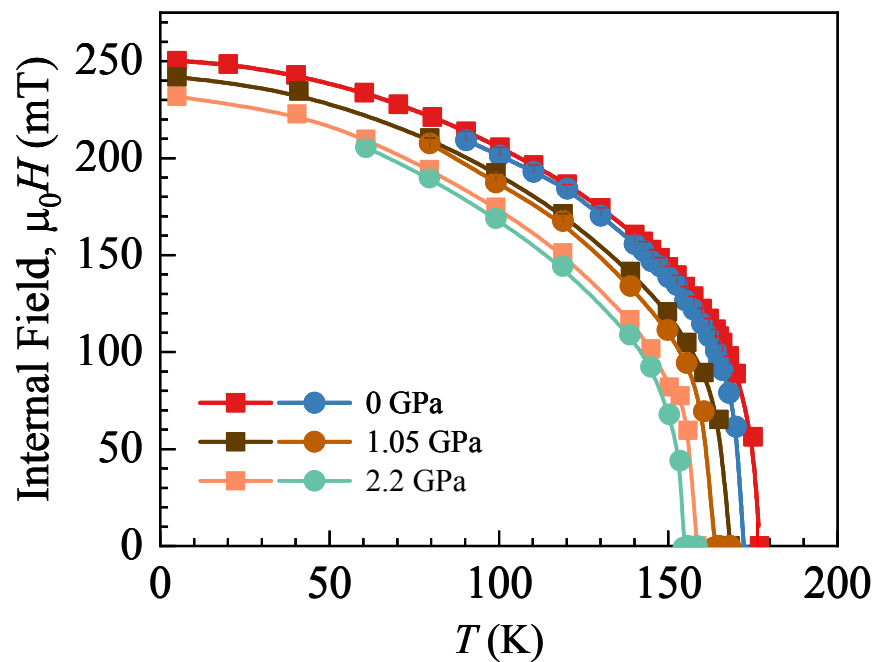
Including all the components and ADPs in the refinement:

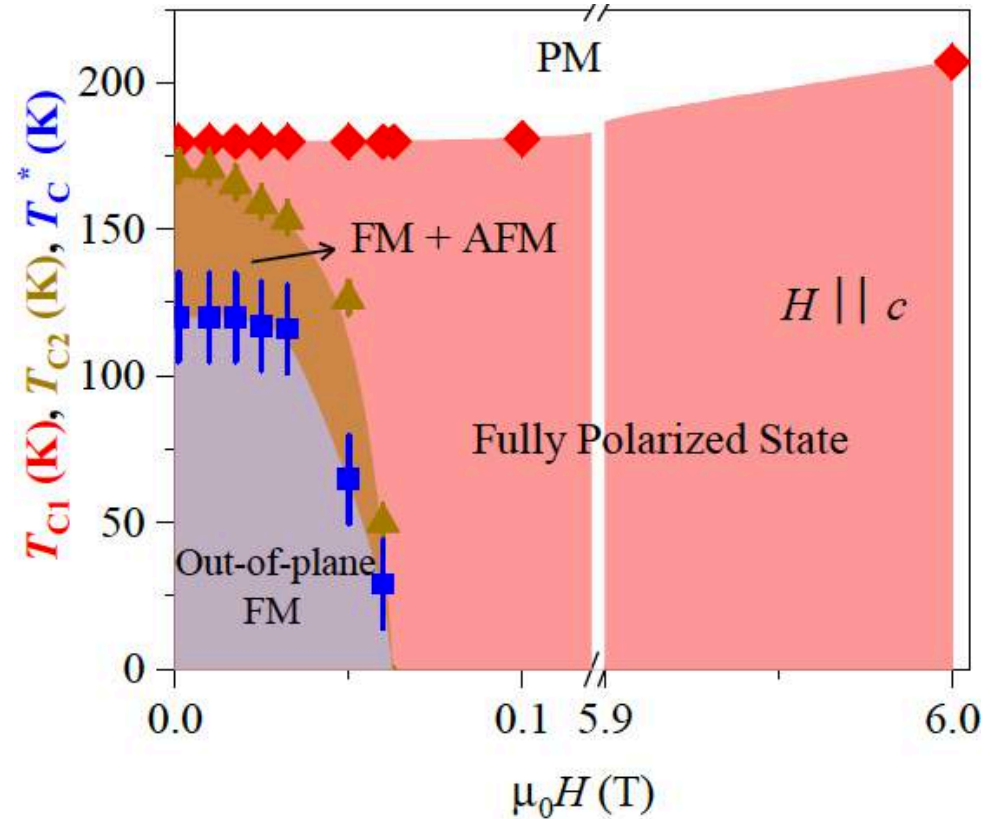
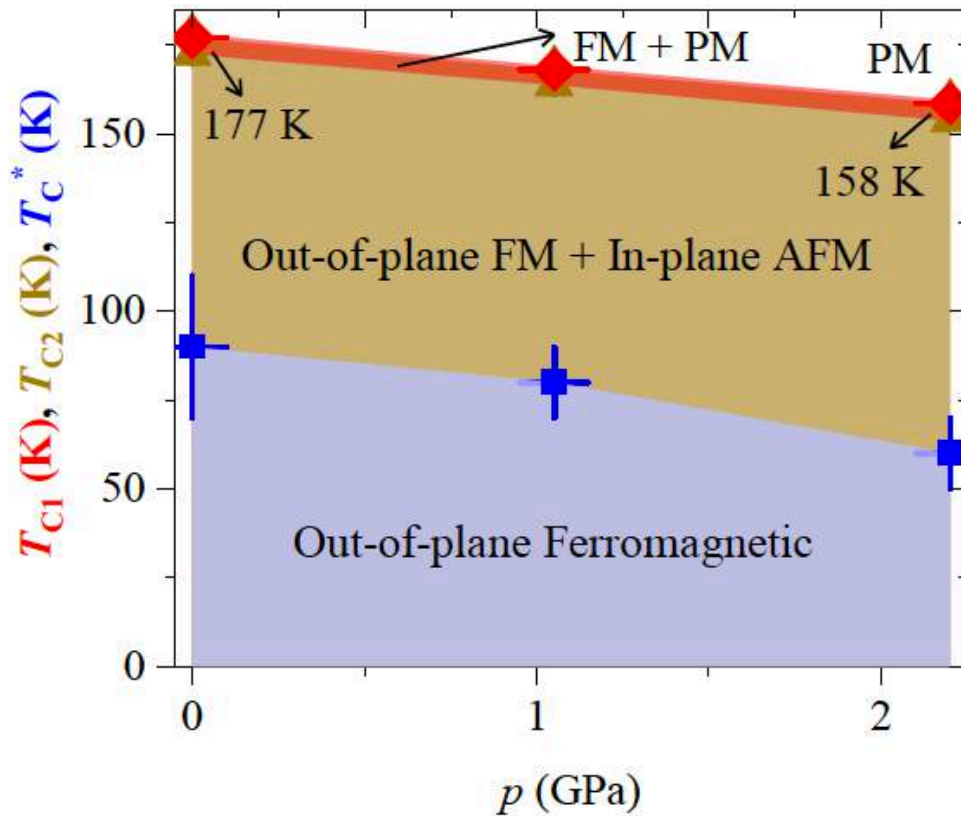
$$\mathbf{M} = (m_x, m_y, m_z) = [0.093(80), 0.187(160), 0.255(137)] \mu_B.$$

Only FM component in the refinement: $m_z = 0.269(102) \mu_B$.



Pressure tuning of magnetic order in $\text{Co}_3\text{Sn}_2\text{S}_2$






- Competition of these magnetic phases is tunable through applying either an external magnetic field or hydrostatic pressure!
- Suggests the quantum tuning of Berry curvature!

Conclusion

- Our experiments suggest that the Co spins have both **FM** order along c-axis and **AFM** order within the kagome plane.
- We present evidence for the **volume wise competition** between these two magnetic orders in the magnetic Weyl semimetal $\text{Co}_3\text{Sn}_2\text{S}_2$.
- The striking **correlation** between the **anomalous Hall conductivity** and the **FM volume fraction**.
- $\text{Co}_3\text{Sn}_2\text{S}_2$ is a rare example where the magnetic competition drives the **thermal (and possibly quantum) evolution of Berry curvature field**, thus tuning its **topological state**.
- The strong interplay between this **intricate magnetism** and the **spin-orbit coupled topological band structure**.

A solid grey square is positioned on the left side of the slide, vertically centered relative to the main text.

**Thank you very much
for your attention!**